

# 1. Unit

As an inter-university research institute, the National Institute for Fusion Science (NIFS) is required to continue to conduct cutting-edge academic research that supports the development of fusion science as interdisciplinary collaborative research, with the active participation of researchers and students from a wide range of fields. To strengthen and expand collaboration between NIFS and universities through interdisciplinary research, a new “Unit System” was established over two years of discussion and founded in FY2023.

Fusion science is an exhaustive research field that aggregates many complex issues. NIFS has the role of realizing collaborative research in coordination with other fields by dividing the challenge of fusion energy into several themes and generalizing each problem. Units are interdisciplinary collaborative research teams that come together under a common research theme, and the Department of Research consists of the following ten Units.

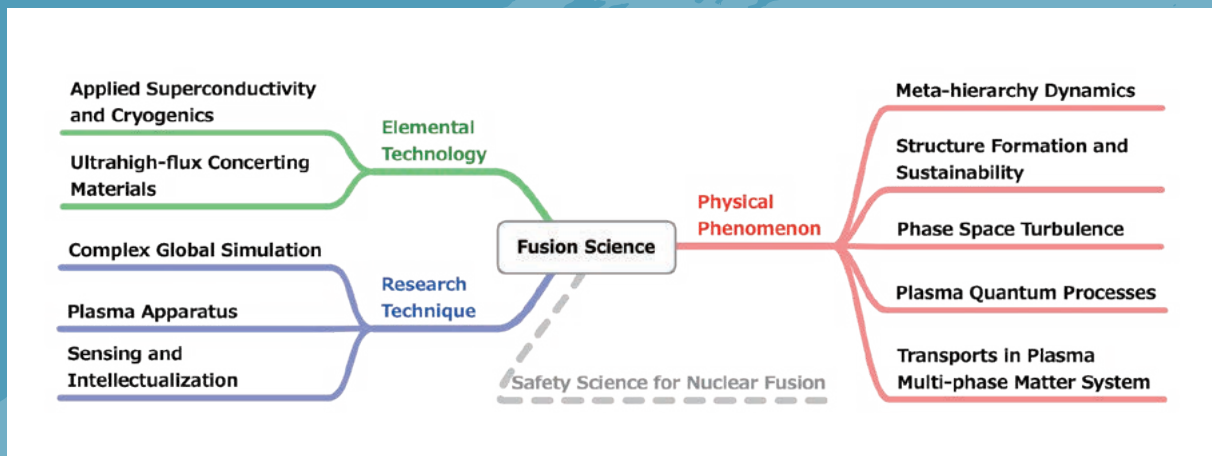


Fig. 1 The Unit System in NIFS. Five Units are focused on physical phenomena, two focus on elemental technology, and three on research techniques. Discussions are continuing on establishing an 11th Unit, “Safety Science for Nuclear Fusion.”

Units are organizations constituting NIFS and are managed in conjunction with the community through the Unit Research Strategy Council, which includes members from outside NIFS. Thus, the community's opinions are directly reflected in the management of NIFS. In addition, many collaborators from universities and research institutions in Japan and overseas participate in the Units' research activities, as shown in the figure.

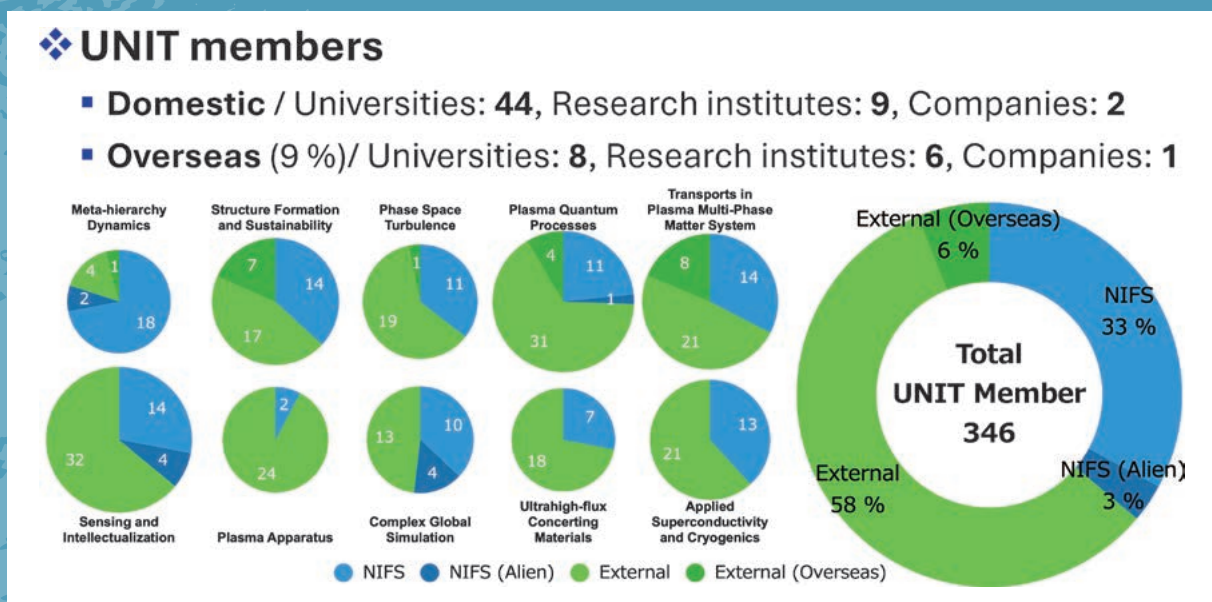


Fig. 2 Composition ratio of Unit members who contribute to arranging an academic plan for the Units from domestic and international universities and research institutions.

The Unit System has established a methodology for conducting cutting-edge academic research that supports the development of fusion science as interdisciplinary collaborative research, with the active participation of researchers and students from various fields.

(R. Sakamoto)

# Meta Hierarchy Dynamics Unit

## Highlight

### Nested invariant tori foliating a vector field and its curl: toward MHD equilibria and steady Euler flows in toroidal domains without continuous Euclidean isometries

We have tackled the challenge of finding a three-dimensional solenoidal vector field where both the field itself and its curl are tangential to a set of given toroidal surfaces. Our approach translates this problem into finding a periodic solution with periodic derivatives for a two-dimensional linear elliptic second-order partial differential equation on each toroidal surface. In the case of magnetohydrodynamics (MHD), the equilibria in a smooth toroidal domain  $\Omega$  are described by magnetohydrostatic (MHS) equations as

$$(\nabla \times \mathbf{B}) \times \mathbf{B} = \mu_0 \nabla P, \quad \nabla \cdot \mathbf{B} = 0 \text{ in } \Omega, \quad \nabla P \times \mathbf{n} = \mathbf{0} \text{ on } \partial\Omega, \quad (1)$$

where  $\mathbf{B}$  and  $P$  are the magnetic field and the pressure, respectively,  $\mu_0$  is the permeability in a vacuum,  $\partial\Omega$  is the bounding surface of  $\Omega$ , and  $\mathbf{n}$  is the unit vector normal to  $\partial\Omega$ . Given a set of nested flux surfaces  $\Psi(x)$ , it has been shown that there exists an integration factor  $\lambda(x)$  and a solenoidal vector field  $\mathbf{B}$  such that  $(\nabla \times \mathbf{B}) \times \mathbf{B} = \lambda \nabla \Psi$  [1]. An example of the result is shown in Fig. 1.

Additionally, we have constructed explicit examples of smooth solutions that are foliated by toroidal surfaces but are not invariant under continuous Euclidean isometries. These solutions are identified as equilibria in anisotropic magnetohydrodynamics.

This investigation addresses a simpler version of a fundamental mathematical problem in MHD and fluid mechanics. Specifically, it concerns the existence of regular equilibrium magnetic fields and steady Euler flows in bounded domains that lack continuous Euclidean isometries. Resolving this problem is crucial for designing confining magnetic fields in nuclear fusion reactors, such as stellarators.

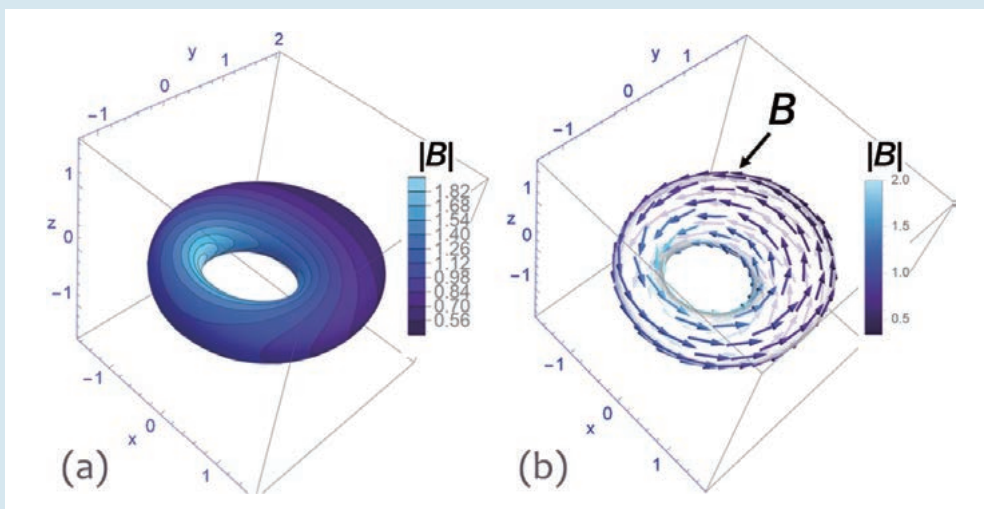


Fig. 1 Example of the result: (a) Contour plot of  $|\mathbf{B}|$  and (b) Vector plot of  $\mathbf{B}$ . Cited from Ref. [1]

[1] N. Sato and M. Yamada, J. Math. Phys. **64**, 081505 (2023).

## Experimental study of the effect of geodesic curvature on turbulent transport in magnetically confined plasma

An experimental study utilizing the Large Helical Device has elucidated the influence of the geodesic curvature of magnetic field lines on turbulent ion-heat transport in magnetically confined plasmas. Statistical analyses, employing the corrected Akaike Information Criterion and multiple regression techniques, have identified geodesic curvature as a significant factor affecting ion-heat transport.

Further evaluation of the geodesic curvature's impact on the zonal-flow effect was conducted using a reduced model based on gyrokinetic simulations. Figure 2 shows the summary of an experimentally obtained data set of the ion-heat transport and turbulence intensity with almost the same non-dimensional parameters. It is seen that the ion-heat transport tends to increase with geodesic curvature. Furthermore, the zonal-flow effect is evaluated and plotted as a function of the geodesic curvature in Fig. 3. This analysis suggests a notable enhancement of the zonal-flow effect when the geodesic curvature is small. Collectively, these independent analyses indicate the potential for external control of zonal flows through manipulation of the magnetic field's geodesic curvature.

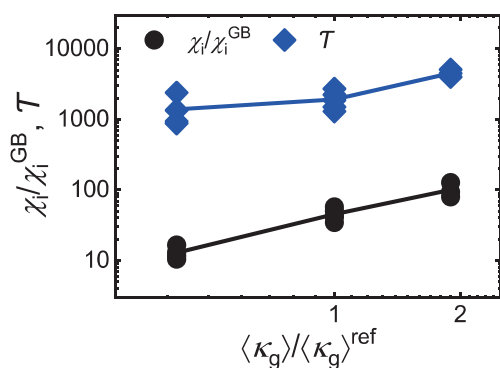


Fig. 2 Normalized ion-heat transport coefficient  $\chi_i/\chi_i^{\text{GB}}$ , and turbulence intensity  $T$  as a function of normalized-geodesic curvature ( $\langle \kappa_g \rangle / \langle \kappa_g \rangle^{\text{ref}}$ ). Cited from Ref. [2].

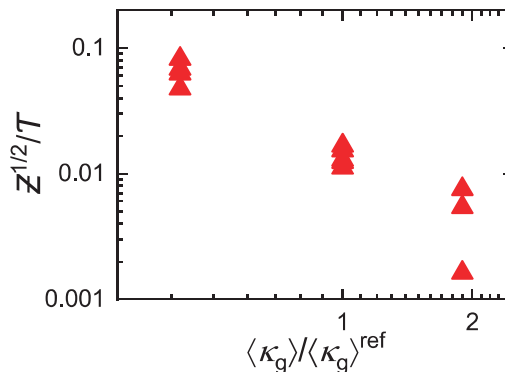


Fig. 3 Zonal-flow effect  $Z^{1/2}/T$  as a function of normalized-geodesic curvature ( $\langle \kappa_g \rangle / \langle \kappa_g \rangle^{\text{ref}}$ ). Cited from Ref. [2].

[2] S. Nishimoto *et al.*, Plasma Phys. Control. Fusion **66**, 04501 (2024).

(K. Nagaoka)

## An Inductively Coupled Plasma System for Investigating Spectropolarimetric Responses of Solar Plasmas to Anisotropic Fields

Accurate measurements and modeling of atomic polarization in three-dimensional radiation transfer are essential for understanding the structure of magnetized solar plasmas. To develop and validate spectropolarimetric measurements and analyses, we have constructed an inductively coupled plasma (ICP) generator specifically designed for plasmas with  $\sim 1$  eV electron temperatures, interacting with radiation and weak magnetic fields. This device was positioned in front of the focal plane of the Horizontal Spectrograph at the Domeless Solar Telescope, Hida Observatory, Kyoto University.

In helium discharges, the electron temperature, electron density, and helium column density of the ICP closely match those found in solar prominences. Comparative spectral analysis reveals nearly identical opacity at He I 1083 nm. By introducing magnetic and radiation fields into the ICP, the system successfully reproduces spectropolarimetric signals as shown in Fig. 4. The results are consistent with those observed in solar prominences [2].

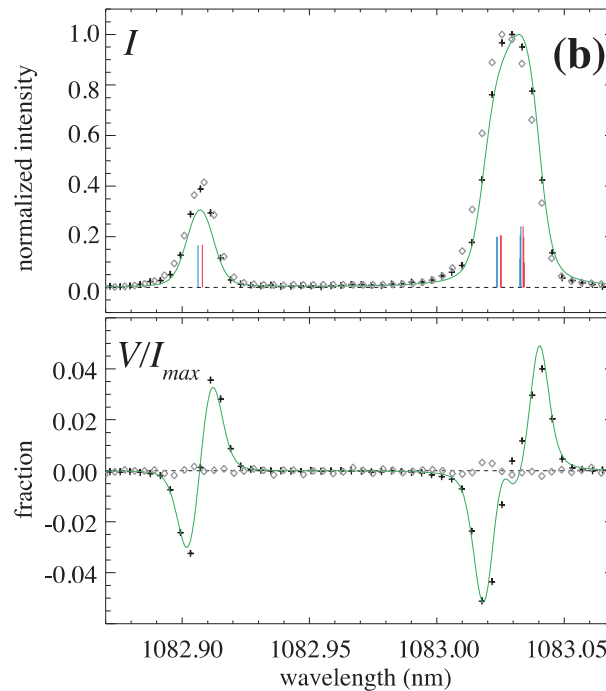


Fig. 4 Normalized intensity  $I/I_{\max}$  and circular polarization  $V/I_{\max}$  from ICP with (black pluses) and without (gray diamonds) magnets under RF power of 100 W and neutral pressure of 5.0 Pa. Blue and red bars show intensities of  $-\sigma$  and  $+\sigma$  components, respectively. Green curves show best fit function. Cited from Ref. [3].

[3] T. Kawate *et al.*, Plasma and Fusion Research **18**, 1401037 (2023).

# Structure Formation and Sustainability Unit

Improving plasma performance and establishing steady-state confinement are central challenges in research to develop fusion reactors that are efficient and compact. The key is to understand the mechanism by which plasmas spontaneously form and maintain their internal structure. When energy is injected into a macroscopic system formed of many components, such as particles, the energy tends to spread among the components. Suppose the system is isolated, meaning there is no energy, momentum, or particle exchange between the system and its environment. In that case, after a sufficiently long time, the system becomes so homogeneous that there is no more “spreading” of energy— it is a maximum-entropy state. However, many systems in the real world are virtually not isolated. In these systems, inhomogeneous structures often emerge and persist. Elucidating the principles that describe structure formation and sustainability in such non-equilibrium systems is one of the biggest challenges of modern science. Fusion science shares this challenge with other research fields, as magnetically confined fusion plasma is a treasure trove of structure formation and self-organization phenomena. Structure formation in plasmas is also common in celestial bodies such as magnetospheres and accretion disks, and is a fundamental concept for understanding the universe. The Structure Formation and Sustainability (SFS) Unit aims to elucidate the principles of structure formation through plasma experiments, theories, and simulations. We comprehensively cover the energy flow through fusion plasma as a system, from the generation of energetic particles to the transport processes that carry energy outside of the plasma. Our research target includes the development of precise measurement of energetic particles and theoretical models/simulations of micro- and macroscopic structure formation, revisiting fundamental physics concepts such as symmetry and entropy production. We are also developing tools to design an innovative fusion reactor. Based on these, we explore the high-performance confinement of fusion plasma.

## Highlight

## Design of new experimental device by advanced optimization technique

Fusion plasma is full of fluctuations of electric and magnetic fields associated with the collective motion of charged particles. These fluctuations are not only considered to be the primary cause of deterioration of plasma confinement but also known to regulate themselves to form ordered structures sustaining confinement. Clarifying the origin and consequence of these fluctuations is critical to developing a compact and efficient fusion reactor. The SFS Unit has started designing a new experimental device to study how collective motion emerges and is regulated in plasma by manipulating the motion of charged particles with a magnetic field. The design process of this device utilizes a new optimization method for the magnetic coils of toroidal fusion devices that the National Institute for Fusion Science has been developing since 2018 [1]. Conventional techniques optimize magnetic configuration and coil shape separately. Our new method optimizes coil shape and the resulting magnetic configuration simultaneously. This new approach enables us to find a coil geometry that can flexibly change the magnetic field while maintaining good plasma confinement. In FY2023, we completed the first conceptual design, confirming that there are coil geometries that realize two types of three-dimensional magnetic configurations with different symmetries, only by changing coil current patterns. Symmetry is an essential parameter of magnetic configuration, as a lack of symmetry can lead to less efficient plasma confinement by complicating the particle motion. Our coil design can realize excellent quasi-symmetry similar to a tokamak and another symmetry similar to a mirror device. We find that the particle motion in these magnetic configurations is drastically different (Fig. 1). We expect that experiments using this new device will open a path to a universal understanding of how the energy of particle motion is converted into collective fluctuations and drives structure formation. Such understanding will contribute to an innovative design of fusion reactors that realizes improved plasma performances.

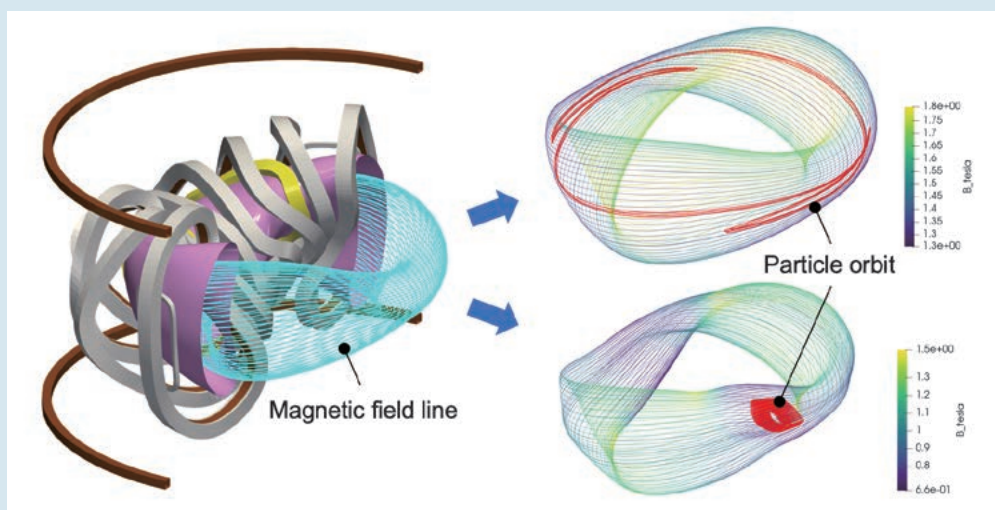


Fig. 1 (Left) the magnetic coils and vacuum vessel of the first conceptual design of a new experimental device (only for a 180° section) and magnetic field line. (Right) typical particle orbit (red curves) in two different magnetic configurations.

(H. Yamaguchi)

## Development of gamma-ray diagnostics for high temporal and energy resolution measurements

Clarifying how often and where fusion reactions occur inside plasma is crucial for deepening the understanding of burning-plasma physics. A useful method to accomplish this is by detecting the radiations emitted by byproducts of fusion reactions. Gamma-ray diagnostics are essential for measuring energy production in burning-fusion plasmas, complementing neutron flux measurements. In fusion research, these diagnostics have been used to measure the temperature of fuel ions and to study the confinement of energetic particles. In the Large Helical Device (LHD), a gamma-ray diagnostic based on an  $\text{LaBr}_3\text{:Ce}$  scintillation detector (Fig. 2), characterized by high detection efficiency and high temporal resolution, was newly installed through a collaboration between the National Institute for Fusion Science, Kyushu University, and Mahasarakham University of Thailand. Mitigating the effects of stray neutrons and gamma rays is key for this new diagnostic system to detect the gamma rays originating from a fusion reaction inside plasma. To this end, we designed shielding based on simulations using the Monte Carlo method. The new diagnostic system worked effectively, and gamma ray spectra were measured in deuterium plasma discharges where hydrogen-beam injection and  ${}^6\text{LiF}$  pellet injection were conducted. A significant peak in the gamma-ray spectrum at approximately 0.48 MeV was observed, most likely due to the fusion reactions between deuterium ions and  ${}^6\text{Li}$  ions ( ${}^6\text{Li}(d,\gamma){}^7\text{Li}$  reaction) inside the plasma. The improvements in the detector performance have extended its operating range and allowed the observation of gamma rays [2]. This is an important step toward experimentally elucidating the behavior of energetic alpha particles produced by fusion reactions.



Fig. 2  $\text{LaBr}_3\text{:Ce}$  scintillation detector

(K. Ogawa)

## Degradation of energetic-ion confinement independent of MHD instabilities is observed.

Neutral beam injection (NBI) is one of the most reliable methods of plasma heating in magnetic confinement fusion devices. Although the total power injected into plasma by a beam injector is measurable, the actual power absorbed in the plasma (in other words, heating efficiency) is not directly measurable. For this reason, estimating energetic-ion loss and clarifying its mechanisms are necessary. In the LHD, deuterium experiments were conducted from 2018 to 2022. Neutron emission due to a fusion reaction between a neutral beam deuterium-ion and a thermal deuterium-ion contains valuable information on how long energetic ions are confined in plasmas. We conducted the deuterium experiments in LHD and simulated the neutron emission rate using the integrated

simulation code TASK3D-a to investigate the energetic ion loss mechanisms. By utilizing the integrated simulation, together with the measured data of neutron emission and impurity-ion density in the deuterium plasma discharges of the LHD, we discovered a confinement degradation phenomenon of energetic ions that had not been recognized before. This degradation, depending on NB power, was observed without the increase in the intensity of magnetic fluctuations associated with magnetohydrodynamic (MHD) activities. Due to this degradation, the neutron emission rate per NBI power decreased by up to 20% after the NBI power was doubled (Fig. 3). We have also found that this degradation is localized around the magnetic axis, which is the center of the plasma. Energetic-ion losses due to MHD activities have been intensively studied as they are concerned with limiting the heating efficiency in fusion reactors in the future. On the other hand, the confinement of energetic ions produced by NBI had been considered to be able to be estimated accurately when MHD activities inside the plasma are negligibly weak. Our discovery of this confinement degradation phenomenon in LHD, enabled by the deuterium experiment, improves the accuracy of predicting energetic ion confinement without MHD activities. This is a basis for obtaining a deeper understanding of MHD-induced energetic-ion losses. Our next step is to identify the mechanisms of this confinement degradation. This research result was published in *Nuclear Fusion*, a journal specializing in fusion science, on April 18th, 2024.

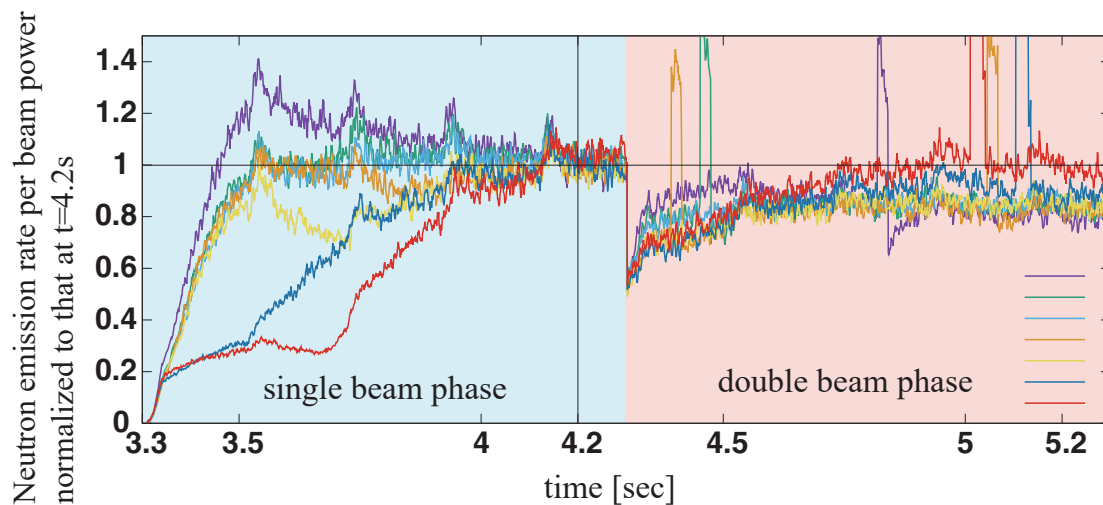


Fig. 3 The vertical axis indicates the neutron-emission rate per beam power normalized to that at  $t=4.2s$ , and the horizontal axis indicates the time from the start of the discharge. The beam power increases by two times after  $t=4.3s$ . Curves in different colors indicate the discharges with different plasma densities. In most discharges, the neutron-emission rate per beam power is reduced by up to 20% after the beam power increases. This reduction reflects the degradation of the confinement of energetic ions.

(H. Nuga)

- [1] H. Yamaguchi *et al.*, “Development of coil-shaping-based optimization code for magnetic fusion devices” 29th IAEA Fusion Energy Conference, TH/P2-14 (2023).
- [2] K. Ogawa, S. Sangaroon, L.Y. Liao, H. Matsuura *et al.*, *Journal of Instrumentation* **18**, P09024 (2023).
- [3] H. Nuga, R. Seki, K. Ogawa, H. Yamaguchi, S. Kamio, Y. Fujiwara, Y. Kawamoto, M. Yoshinuma, T. Kobayashi, Y. Takemura, M. Isobe, M. Osakabe and M. Yokoyama, “Degradation of fast-ion confinement depending on the neutral beam power in MHD quiescent LHD plasmas”, *Nuclear Fusion* **64**, 066001 (2024).

# Phase Space Turbulence Unit

## Phase-space tomography

Magnetically confined fusion plasmas are generally very low in density, so particle collision rarely occurs. Particles have electric charges therefore can be trapped or expelled in a phase of electrostatic waves. Those trapped particles travel with the waves while being bounced by wave potential, like surfing (Fig. 1). During this motion, the waves and particles can exchange their energy and momentum, leading to more complicated behaviors. As a result, different nonlinear phenomena that significantly impact on plasma confinement can occur: for example, enhanced-plasma transport that makes the plasma confinement worse and collisionless plasma heating. So far, direct observation of those wave-particle interactions has been extremely challenging and therefore experimental knowledge obtained is limited. A key quantity is the velocity distribution function, which describes statistical properties of particle dynamics. In a non-fluctuation situation the velocity-distribution function follows Gaussian (normal) distribution.

One of the issues that makes phase-space structure measurement challenging is the trade-off relationship between time, real-space, and velocity-space resolutions and signal intensity. As the total signal intensity that is determined by the diagnostic system and plasma condition is constant, improving resolution results in a decrease of signal intensity at a single detector pixel [1].

Recently, a new signal processing algorithm has been proposed to overcome the trade-off relationship between resolutions and signal intensity, that is, phase-space tomography [2]. In this algorithm, a set of three integrated signals with the same viewing sight is used to recover three-dimensional resolution in phase-space. Integrations are performed in each dimension, i.e., time, real-space, and velocity-space. As a tomography technique, the maximum likelihood expectation maximization (MLEM) method is used. For test data generated according to an LHD observation, it was proven that the proposed method reasonably recovered the resolution from a set of integration data through this algorithm.

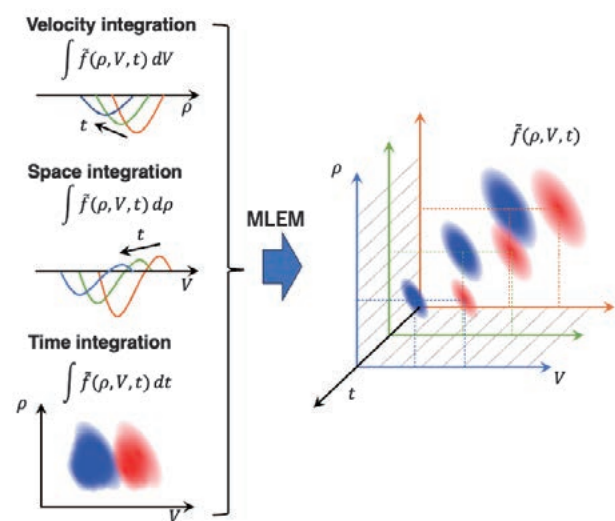


Fig. 1 Schematic of phase-space tomography

- [1] T. Kobayashi, "Prospect for experimental investigation of phase-space turbulence in magnetically confined fusion plasmas", *Plasma and Fusion Research* **18**, 2402059 (2023).
- [2] T. Kobayashi, M. Yoshinuma, W. Hu, K. Ida, "Phase-space tomography in magnetically confined plasmas", *Physics of Plasmas* **30**, 052303 (2023).

(T. Kobayashi)

## First demonstration of predictive control of fusion plasma by digital twin: application of data assimilation to adaptive predictive control

Fusion energy, particularly through magnetic confinement, is a promising solution to global energy problems. This method involves confining high-temperature plasma within a reactor using a magnetic field to convert fusion energy into electricity. Predicting and controlling the complex behavior of fusion plasma is essential for success. One approach, digital twin control, uses a simulated plasma to guide the actual plasma control. This is challenging due to the need to consider factors like plasma flow, heating, fuel supply, impurities, and neutral particles, along with limited measurement capabilities in future reactors.

A new control system to optimize predictive models using real-time observations has been developed in collaboration with the Phase Space Turbulence Unit, the Structure Formation and Sustainability Unit, the Sensing and Intellectualizing Technology Unit, the Plasma Quantum Processes Unit, and the Complex Global Simulation Unit. This system, called ASTI (Assimilation System for Toroidal Plasma Integrated Simulation), employs data assimilation to improve the accuracy of numerical simulations by incorporating observed data. ASTI adapts the simulation model to the actual behavior of the fusion plasma in real time, allowing for accurate predictions and control. It performs numerous parallel simulations to probabilistically predict the plasma's future state, adjusting to real plasma observations and target states for optimal control estimation. This system was tested on the Large Helical Device (LHD), a leading superconducting plasma experimental facility. An experiment to control the electron temperature of the plasma using electron cyclotron resonance heating (ECH) demonstrated the successful predictive control of fusion plasma by a digital twin, based on data assimilation. The electron temperature was brought close to the target while improving the prediction accuracy, marking a world-first achievement. This control approach is expected to be fundamental for fusion reactor control, addressing issues like plasma density and temperature-profile control and controlling quantities not directly measured.

The development of the control system represents a significant step toward advanced controls necessary for fusion power generation. Future plans include expanding the control system and conducting more advanced demonstrations at the LHD and other experimental devices worldwide. This data assimilation-based method provides a foundation for adaptive-predictive control in scenarios where high accuracy prediction by simulation alone is difficult. It also has potential applications in solving complex societal issues with many uncertain factors, such as road traffic control and river water level management.

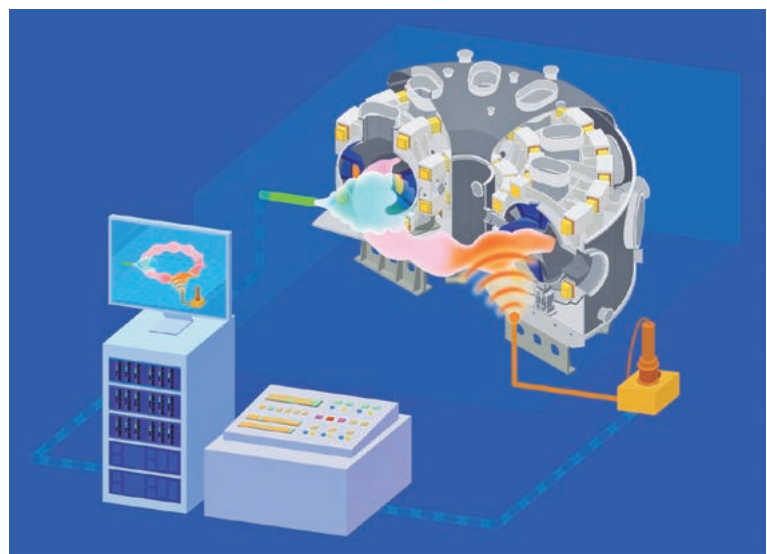


Fig. 1 Image of digital twin control, in which real plasma is controlled by virtual plasma reproduced on a computer.

[1] Y. Morishita *et al.*, *Scientific Reports* **14**, 137 (2024).

# International joint research for development of output power of 1 MW with a 35 GHz gyrotron

In FY2022, we agreed a research partnership with Kyoto Fusioneering, a fusion start-up company, to collaborate on “research on the long pulse of high-power gyrotrons, etc.” As part of this joint research, we focused on developing a beam oscillation and transmission system for a gyrotron operating at low frequencies (28 GHz/35 GHz). This system will be utilized for plasma heating and current-drive experiments in the MAST-U fusion spherical tokamak device at UKAEA. Since high-power oscillation and transmission in this low-frequency range is unprecedented, we needed to develop the gyrotron and its associated components. We tested a dual-frequency gyrotron tube designed for a nominal-beam output of 1 MW-3 s and its peripheral components for testing at our institute. We conducted magnetic field measurements with a superconducting magnet (Fig. 1), installed and adjusted the gyrotron (Fig. 2 left), performed mode-purity measurements of the output beam at the exit of the gyrotron and after passing through mode matching unit (MOU) (Fig. 2 right), and carried out high-power and second-order oscillation tests. The dual-frequency gyrotron successfully achieved the output of 1 MW-3 s. Once developed, the gyrotron will be shipped to the UK for plasma experiments to gather valuable information for the design of future power plants and to address physics challenges.



Fig. 1 Magnetic field measurements carried out prior to installation of the gyrotron.

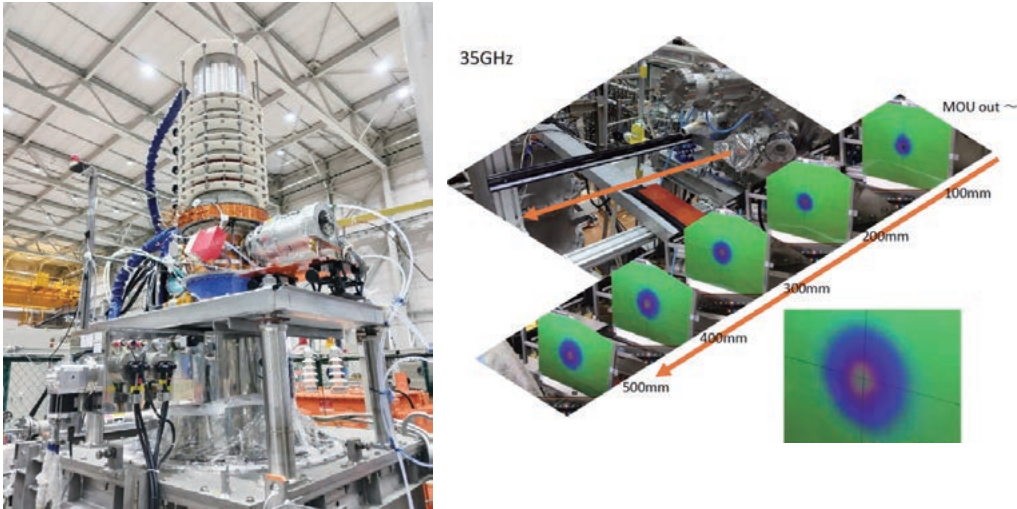


Fig. 2 A dual frequency gyrotron installed for oscillation and transmission testing (left figure). Output beam after passing the MOU. The expected Gaussian beam shape was obtained (right figure).

[1] Press release, Kyoto Fusioneering, National Institute for Fusion Science, Tsukuba University, UK Atomic Energy Authority, CANON ELECTRON TUBES & DEVICES, January 12, 2024, <https://www.nifs.ac.jp/news/collabo/240112.html>

Expert contact. M. Nishiura

[2] Newspaper interview, “Road to Compact of Fusion Reactor”, Gifu Shinbun, morning newspaper, page 3, February 10 2024.

(M. Nishiura)

# Plasma Quantum Processes Unit

The goals of the Plasma Quantum Processes Unit are to advance interdisciplinary plasma research based on quantum processes, and to promote international collaborations. Toward these goals, each member of the Unit is pursuing research with the following academic strategies.

## Advancement

- Advancement of plasma measurement based on highly-charged ion spectroscopy/quantum processes
- Inclusion of quantum physics in plasma kinetics and enhancement of accuracy of kinetic transport calculations including highly-charged ions
- Fusion reactor edge plasma modeling, including atomic and molecular processes and plasma-wall interactions

## Interdisciplinary

- Collaboration with other fields using atomic and molecular data/promoting applications by developing databases
- Research on ultra-relativistic plasma dynamics, including quantum electrodynamics processes, and development of laboratory astrophysics using intense lasers
- Promoting collaboration with other units and interdisciplinary research with physics fields other than fusion, from the viewpoint of data-driven science and materials informatics for advanced measurements
- Interdisciplinary collaboration with particle-physics fields through research on quark-gluon plasma, and obtaining hints for new measurements in fusion-plasma experiments from detectors in high-energy accelerator experiments
- Applying cryogenic engineering technology developed in fusion research to high-energy density sciences

To ensure that the Unit's research activities are carried out with the participation of the broader academic community, a Unit Research Strategy Council was organized, inviting 15 external members from various research fields.

The unit regularly holds seminars with external collaborators to disseminate its research activities. From April 2023 to March 2024 ten seminars were held on relevant topics, i.e. highly-charged ion spectroscopy, data-driven sciences, quark-gluon plasmas, X-ray imaging and Spectroscopy Mission (XRISM), neutron star mergers and kilonovae, and intense laser-matter interaction and its applications.

Workshops and seminars for "2DMAT," a data-driven software framework developed in collaboration with ISSP, University of Tokyo, were organized to facilitate its applications to advanced plasma measurements.

The unit is developing numerical databases of atomic and ion-surface collisions for fusion and plasma applications by international collaborations. The databases are available on the internet (<https://dbshino.nifs.ac.jp/index-j.html>).

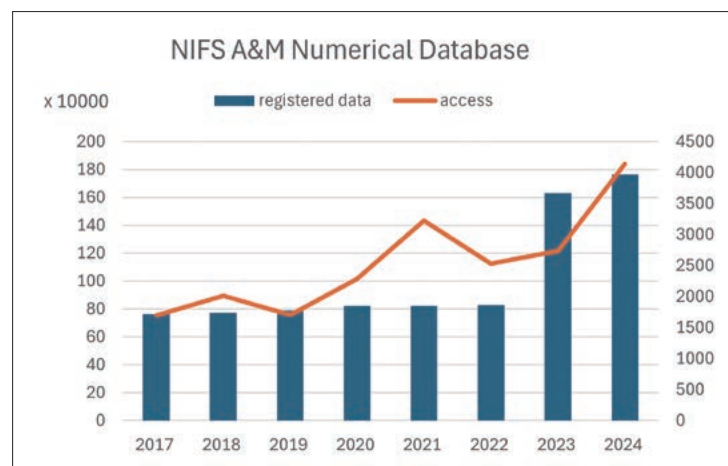


Fig. Annual changes in the number of registered data (left) and access (right) to the NIFS database. The numbers are shown until April of each year.

(D. Kato)

## Highlight

## Spectroscopy study of $\text{Kr}^{25+}$ ion for krypton seeding experiment in the Large Helical Device [1]

A krypton gas impurity seeding experiment was conducted in the Large Helical Device. Emission lines from Na-like Kr ions in the extreme ultraviolet wavelength region, such as 22.00 nm, 17.89 nm, 16.51 nm, 15.99 nm, and 14.08 nm were observed. A suitable Collisional-Radiative (CR) model was developed to produce the synthetic spectrum of the  $\text{Kr}^{25+}$  ion. For this, the relativistic multiconfiguration Dirac–Hartree–Fock method was employed, along with its extension to the Relativistic Configuration Interaction (RCI) method for atomic structure calculations using the General Relativistic Atomic Structure Package-2018. In addition, another set of calculations was carried out utilizing the relativistic many-body perturbation theory and RCI methods integrated within the flexible atomic code. In addition, we undertook calculations of the cross-sections for the fine structure transitions of the  $\text{Kr}^{25+}$  ion using the relativistic distorted wave method [1]. We incorporated important electron impact excitation processes, along with their reverse processes in the CR model. Rate-balance equations were solved simultaneously for an electron temperature of 600 eV and an electron density of  $6 \times 10^{19} \text{ m}^{-3}$ . To validate our findings, the emission lines measured in the experiment, were compared with the CR model spectrum and shown in Figure 1. Our comparative analysis revealed an overall good agreement with the CR model calculations.

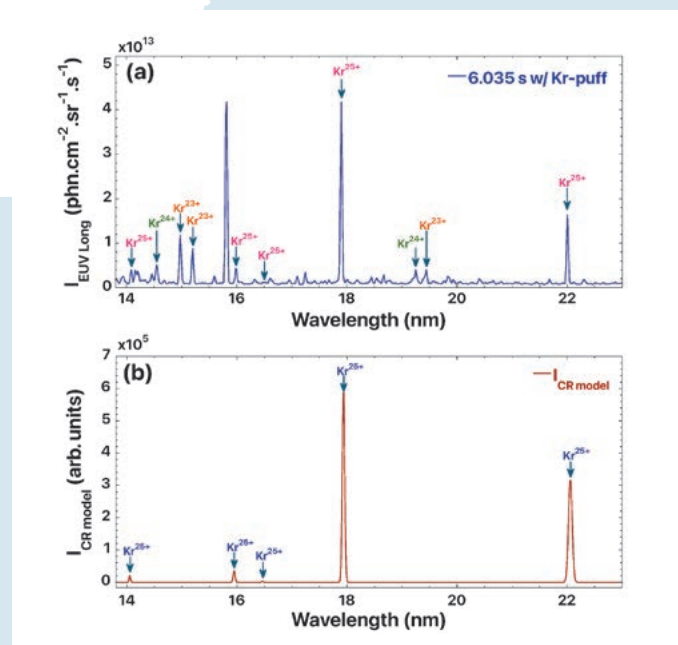


Fig. 1 (a) Experimental extreme ultraviolet spectrum of highly-charged Kr ions (14–23 nm) in the LHD, (b) comparative synthetic  $\text{Kr}^{25+}$  spectrum from the CR model

[1] S. Gupta, T. Oishi, I. Murakami, “Study of Electron Impact Excitation of Na-like Kr Ion for Impurity Seeding Experiment in Large Helical Device” *Atoms*, **11**, 142 (2023).

## Highlight

## Abnormal ionization equilibrium mediated by long-lived metastable excited states [1]

The charge-state distribution of atomic ions in plasmas is fundamental to various plasma applications. For instance, industrial applications using highly-charged ions, e.g., an extreme-ultraviolet light source based on a laser-driven plasma, should maintain efficient production of the objective charge-state ions. The population distribution of charge states also provides crucial information for plasma diagnostics because it generally depends on the plasma condition. In particular, the electron-temperature dependence of the abundance ratio between neighboring charge states (higher to lower) generally shows a monotonical increment with increasing electron temperature. This general behavior is advantageous for plasma diagnostics of astrophysical and fusion plasmas. It is also useful for emission-line assignments, since the charge state of the ions can be easily identified by observing the electron temperature (energy) dependence of line intensities in a laboratory plasma.

In our recent activity on highly-charged ion spectroscopy using a compact electron beam-ion trap (CoBIT), we experimentally found that the above general behavior does not hold in some cases. The electron energy dependence of the line intensity ratio of  $\text{Ba}^{10+}/\text{Ba}^{9+}$  decreases with increasing electron energy in a particular energy region, implying there is a characteristic electron energy dependence of each ion abundance. We successfully reproduced the experimentally observed characteristic behavior using a state-of-the-art theoretical simulation based on fine-structure-resolved collisional-radiative modeling with ionization balance. The calculation results suggested that this anomalous behavior was caused by indirect plasma ionization processes from metastable states in  $\text{Ba}^{9+}$  and  $\text{Ba}^{8+}$ . The present study provides a new insight into plasma physics relevant to highly charged ions.

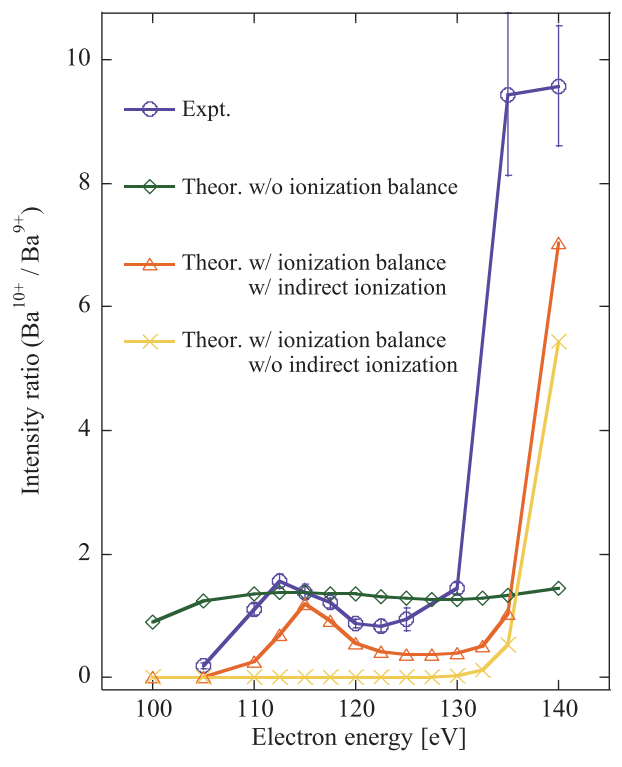


Fig. Electron-energy dependence of the intensity ratio between the extreme ultraviolet emission lines of  $\text{Ba}^{10+}$  and  $\text{Ba}^{9+}$ .

[1] N. Kimura, Priti *et al.*, "Anomalous plasma ionization balance induced by 5s and 4f metastable states", *Physical Review A* **108**, 032818 (2023).

(N. Kimura, Tokyo University of Science)

## Highlight

## Improvement of electron temperature and density accuracy in Thomson scattering diagnostics by an accumulation of 100 laser pulses within 5 milliseconds [1]

In electron temperature ( $T_e$ ) and density ( $n_e$ ) measurement by Thomson scattering diagnostics for high  $T_e$  and low  $n_e$  plasmas, scattered light intensity is usually small because the total intensity of the scattered light and the Doppler broadening of the spectrum are related with  $n_e$  and  $T_e$ , respectively. In order to improve this, the signals from multiple laser pulses are accumulated. A Nd:YAG laser with a high repetition rate of up to 20 kHz is used in the Thomson scattering system in the LHD. In a 20 kHz operation, 100 laser pulses, each of which has almost 1 J of pulse energy, were irradiated in 5 ms with intervals of 50  $\mu$ s. This method was tried for a plasma with  $n_e$  lower than  $2 \times 10^{18} \text{ m}^{-3}$  and almost in a steady state during this time range. The S/N ratio in raw signals by one laser pulse seems to be almost in the order of one. When more than ten signals are summed, the signal components become clear. Although the background level is important for the integration of the signals in time, it is still affected by noise in the case of the summation of the ten signals. The effect of the noise seems to disappear in the case of the summation of 100 signals. Figure 1 shows the spatial profiles of  $T_e$  (red) and  $n_e$  (blue) from (a) 1 signal, (b) 10 signals and (c) 100 signals. In Fig. 1 (a), the magnitude of  $T_e$  error is large and the  $T_e$  data are scattered. In Fig. 3 (c), the magnitude of error near the center is smaller than in (b). In this plasma,  $T_e$  around the center region is evaluated to be more than 15 keV, by averaging of the Thomson scattered signals from 100 laser pulses which are injected into the plasma within 5 ms.

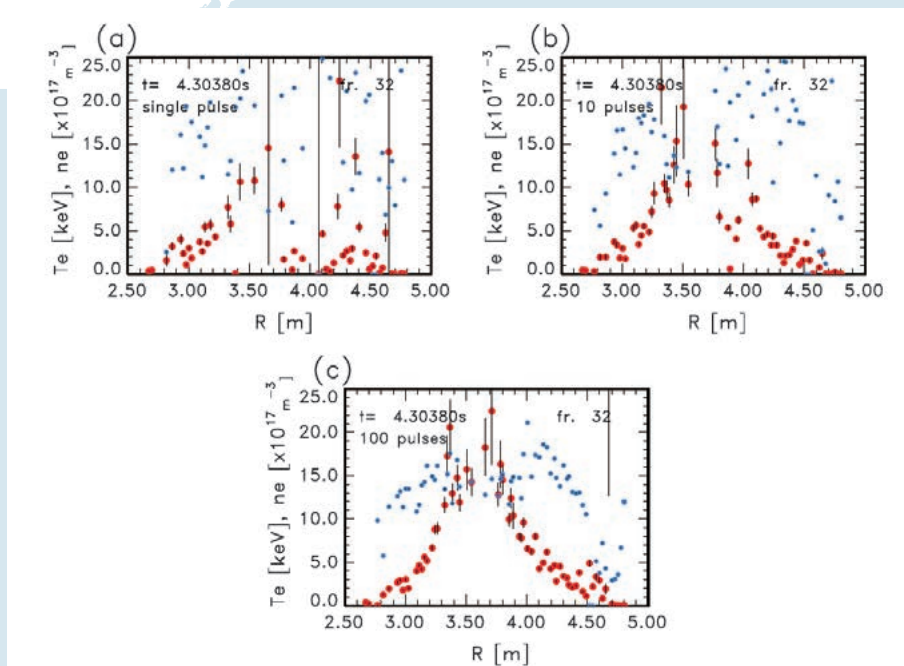


Fig. 1 The red closed circles show the  $T_e$  profile and the blue closed circles show the  $n_e$  profile. (a) Data by a single laser pulse is used. (b) Signals of ten laser pulses are averaged. (c) Signals of 100 laser pulses are averaged. [1]

[1] H. Funaba *et al.*, Journal of Instrumentations **18**, C11015 (2023).

## Highlight

## Experimental investigations on space and astrophysical plasmas with lasers: magnetic reconnection in complex magnetic fields

The underlying physics of space and astrophysical phenomena has been investigated using scaled laboratory experiments, which is referred to as “laboratory astrophysics” in the field of laser-produced plasmas. In this fiscal year, we published an international collaborative paper with Japan, Taiwan, Czechia, and Indonesia on the structure formation during electron-scale magnetic reconnections in self-generated and external magnetic fields, using laser-produced plasmas [1]. We performed an experiment with complex magnetic-field lines due to two origins of the magnetic field: self-generated (Biermann battery) and external magnetic fields. Both magnetic fields formed anti-parallel magnetic-field configurations to drive magnetic reconnections. The emission images of plasma expansion in the presence and absence of the external magnetic field are compared in Fig. 1. In the absence of the external magnetic field in Fig. 1 (a), the plasma vertically expands at  $x \sim 6$  mm, which is a typical structure generated by magnetic reconnection in Biermann magnetic fields. The image with the external magnetic field in Fig. 1 (b) shows the horizontal separation of the plasma at  $x \sim 4$ –5 mm, which is a signature of the magnetic reconnection in the external magnetic field. There is a vertical expansion with the external magnetic field; however, the signal intensity is weaker than that without the external magnetic field. This indicates that the magnetic reconnection in the self-generated magnetic fields can be suppressed in the presence of the external magnetic field. As a step beyond this, we are planning to investigate the connection between electron to magnetohydrodynamic (MHD) scales, using a co-creation platform of magnetic fields and lasers.

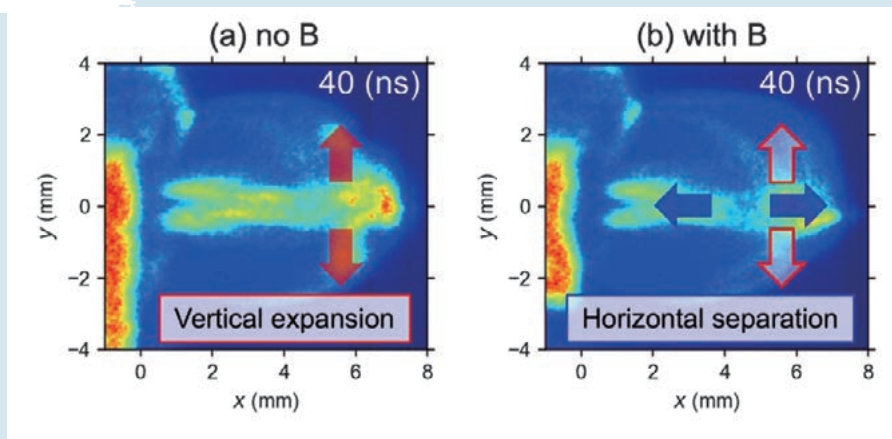


Fig. 1 Self-emission images of the plasma expansion obtained at 40 ns after the irradiation of the drive laser pulse (a) without and (b) with the external magnetic field.

[1] K. Sakai *et al.*, “Competition of magnetic reconnections in self-generated and external magnetic fields” *High Energy Density Phys.* **52**, 101132 (2024).

## Highlight

## Transition Probabilities of Near-infrared Ce III Lines from Stellar Spectra: Applications to Kilonovae [1]

Coalescence of binary neutron stars (NSs) is the promising site for the rapid neutron capture nucleosynthesis and thus for the origin of heavy elements in the universe. In 2017, associated with the detection of gravitational waves from an NS merger (GW170817), thermal emission powered by the radioactive decay of freshly synthesized nuclei in NS-merger ejecta (“kilonova”) was observed in ultraviolet, optical, and near-infrared (NIR) wavelengths. The observational properties of the kilonova provided us with evidence that the NS merger is a site where heavy elements are produced.

Nevertheless, a detailed abundance pattern, i.e., the species and amounts of synthesized elements is not clear and an important subject to study. One of the direct ways to find the synthesized elements is the identification of absorption lines in the observed spectra of a kilonova. Domoto et al. [2] have reported that one of the absorption features in the observed NIR spectra of the kilonova can be explained by the lines of Ce III. However, due to a lack of experimental data, they used theoretical transition probabilities (gf-values) of the Ce III lines whose accuracy is uncertain [3].

To verify this identification, in the present study [1], we derived the gf-values of three Ce III lines by utilizing stellar spectra showing Ce III absorption as a plasma laboratory. We modeled high-resolution NIR spectra of four stars by assuming the stellar parameters derived from optical spectra in the literature. We found that the derived values were broadly consistent with the theoretical values available from literature, within the uncertainties. We confirmed that the absorption features by Ce III appeared in the spectra, even considering the uncertainties in the derived gf-values. This supports the identification of Ce in the observed spectra of the kilonova.

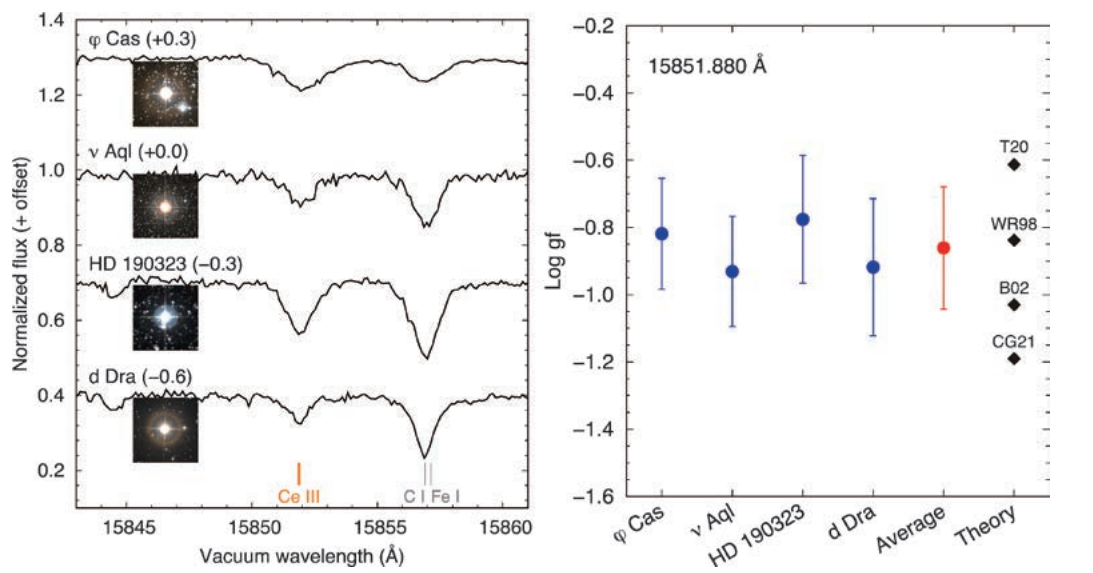


Fig. 1 Left: the stellar spectra used for this work, focusing on one of the Ce III lines (at 15851.880 Å). The position of the Ce III line is indicated by the orange line. The names and images of the stars are also shown. Right: the gf-values of one of the Ce III lines (at 15851.880 Å) derived from the four stars (blue), and their average as the final result (red). Black diamonds show the theoretical values available from literature.

- [1] N. Domoto *et al.*, “Transition Probabilities of Near-infrared Ce III Lines from Stellar Spectra: Applications to Kilonovae” *Astrophys. J.* **956**, 113 (2023).  
 [2] N. Domoto *et al.*, “Lanthanide Features in Near-infrared Spectra of Kilonovae” *Astrophys. J.* **939**, 8 (2022).  
 [3] M. Tanaka *et al.*, “Systematic opacity calculations for kilonovae” *Mon. Not. R. Astron. Soc.* **496**, 1396 (2020).

(N. Domoto, Tohoku University)

# Transports in Plasma Multi-phase Matter System Unit

The research aims of this Unit are: to understand, predict, and control heat, particle, and momentum-transport phenomena in systems where plasma contacts solids, liquids, and gases from the open magnetic field region of a magnetic confinement fusion reactor to the wall, coolant, exhaust system, and the fuel circulation system; to apply the knowledge and techniques gained from the studies mentioned above to various fields outside fusion, contributing to their advancement.

Here, the results obtained from research in this Unit and published as papers in FY2023 are introduced.

## Simulation analysis of the ablation positions of boron dust particles dropped from the impurity powder dropper in LHD [1]

Control of the ablation positions of boron dust particles dropped from an Impurity Powder Dropper (IPD) is critical for effective real-time boronization. The movement of the ablation positions of dust particles toward the outboard side of the torus has been observed with an increase in plasma density. Figure 1 (a) presents fast-framing camera observations of the ablation of the dropped boron dust particles for two different line-averaged plasma densities  $\bar{n}_e$  of 1 and  $5 \times 10^{19} \text{ m}^{-3}$ , showing that the ablation position moved toward the outboard side with the plasma density. A dust particle transport simulation using the DUSTT code successfully reproduced the observations. Figure 1 (b) illustrates a simulation of the dropped dust particle trajectories in background plasmas with three different plasma densities at the Last Closed Flux Surface  $n_e^{\text{LCFS}}$  of 1, 2, and  $4 \times 10^{19} \text{ m}^{-3}$ , in which three-dimensional plasma parameter profiles were calculated by the EMC3-EIRENE code. The simulation revealed that the dropped dust particle trajectories were deflected toward the divertor plates at an upper divertor leg by the effect of the plasma flow. It also shows that the plasma-flow effect increased with the plasma density, resulting in the movement of the ablation positions toward the outboard side.

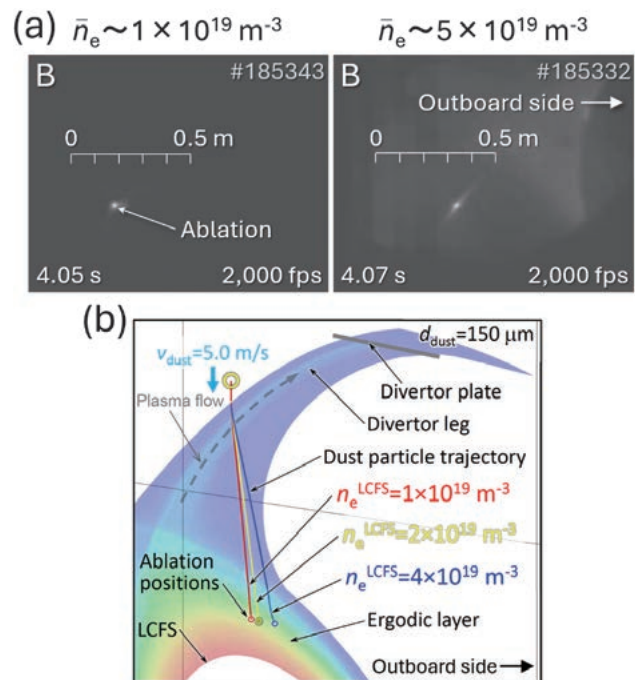


Fig. 1 (a) Images of the ablation of the dropped boron dust particles observed with a fast-framing camera for two different line averaged plasma densities  $\bar{n}_e$  of 1 and  $5 \times 10^{19} \text{ m}^{-3}$ . (b) the simulations of the dropped dust particle trajectories in background plasmas with three different plasma densities at the Last Closed Flux Surface  $n_e^{\text{LCFS}}$  of 1, 2, and  $4 \times 10^{19} \text{ m}^{-3}$ .

(M. Shoji)

## Ultra-high neutral pressure achieved in the divertor [2]

For the first time, a very high neutral pressure in a divertor region has been observed in a high-density experiment in the Large Helical Device (LHD). The divertor plays a role in removing impurities and improving particle control by increasing the number of neutral particles inside and efficiently exhausting them. Previous research has shown that hydrogen-neutral particles can be highly compressed inside the divertor (Fig. 2 (a)) if the position of the center of the plasma (magnetic axis) is inwards. However, this time the magnetic field configuration was shifted to 3.55 m, only 5 cm inwards from the magnetic axis condition (3.60 m), which is commonly used. As shown in Fig. 2 (b), a neutral pressure more than seven times higher was achieved. One of the possible reasons for this was that the plasma inside the divertor was relatively cold, a condition known as volume recombination, and the research team named the ultra-high neutral pressure phenomenon inside the divertor “low-temperature mode”. The present results mean that the neutral pressure inside the divertor can be increased by optimization of the magnetic field configuration, which provides important insights for the design of fusion DEMO reactors.

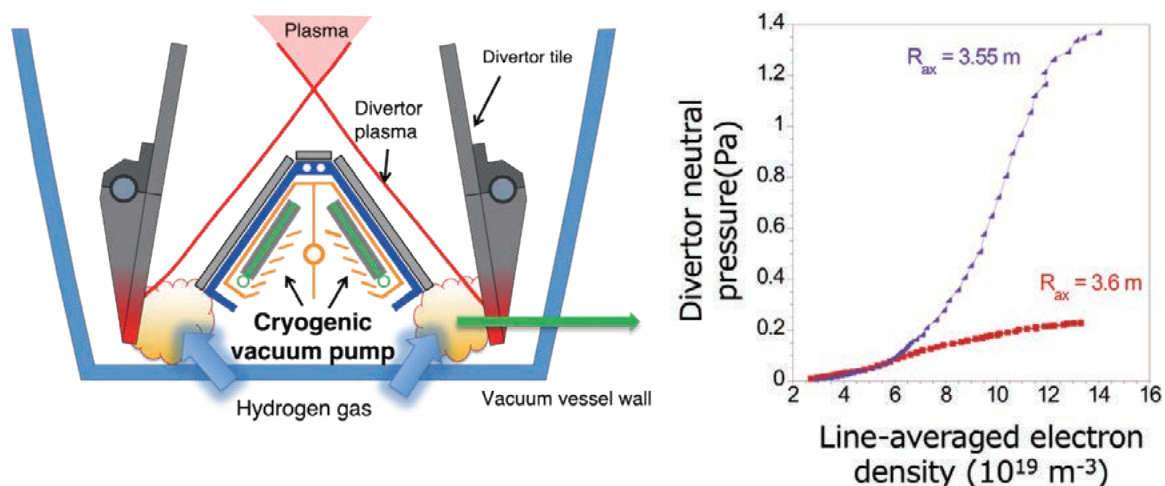


Fig. 2 At the edge of the plasma confined by the magnetic field in the Large Helical Device (LHD), the plasma is drawn into a region called the divertor system, where the plasma becomes neutral gas. In this achievement, a very high neutral pressure of 1.4 Pa is achieved in a specific magnetic field configuration.

(U. Wenzel and G. Motojima)

## Plasma-wall interaction (PWI) on a new type of divertor-heat removal component in LHD [3]

A novel method, called Advanced Multi-Step Brazing (AMSB), has been developed to fabricate a new type of divertor heat removal component with W armor and an oxide-dispersion-strengthened copper (GlidCop®) heat sink. A new type of divertor-heat removal component, which has a rectangular-shaped cooling channel with a V-shaped staggered-rib structure in the GlidCop® heat sink, has been developed. The new component was installed in the divertor-strike position of the Large Helical Device (LHD), as shown in Fig. 1 and exposed to neutral beam injection-heated plasma discharges with 1180 shots (~8000 s) in total. Fig. 3 shows a photograph of

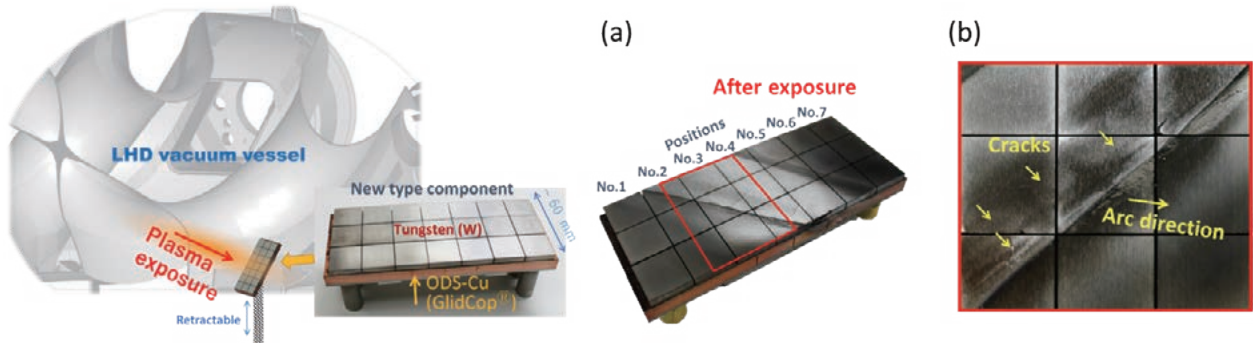


Fig. 3 (left) Schematic view of experimental set-up for irradiation of the new type of divertor heat removal component in LHD. (a) Photograph of the new type of divertor heat removal component after exposure to LHD divertor plasma. (b) Enlarged image of W surface corresponding to red rectangular area of photograph (a).

the exposed component. Though submillimeter-scale damage, such as unipolar arc trails and microscale cracks, was identified on the W surface, the extremely high heat removal capability did not show any sign of degradation over the experimental period. On the other hand, remarkable sputtering erosion and redeposition phenomena, due to the strong influx of the divertor plasma, were confirmed on the W armor.

(M. Tokitani)

## OL impurity transport analysis with SONIC code with a kinetic effect on a thermal force transport model in JT-60U [4]

The latest version of the SONIC code, edge plasma transport simulation code, with an extended thermal force model, which is capable of treating collisionality dependence of the force, has been applied to JT-60U plasmas to investigate the kinetic effect on the scrape-off layer (SOL) impurity transport [4]. It is found that maximum

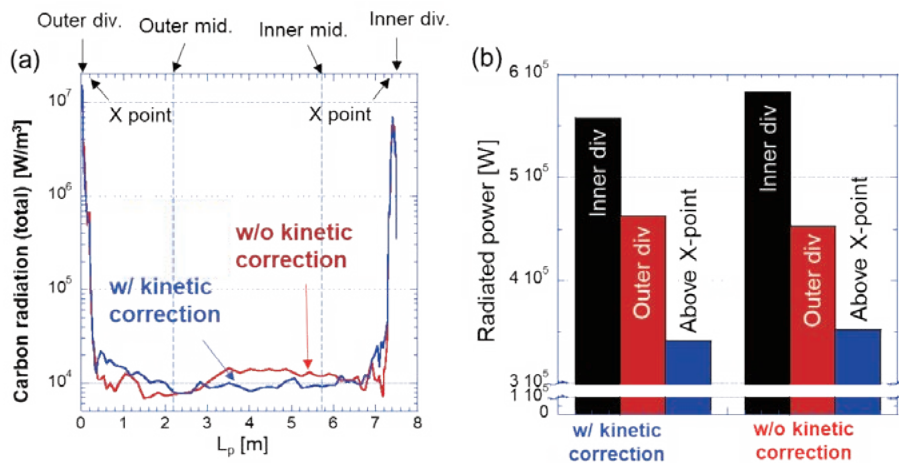


Fig. 4 (a) Impurity radiation profiles along magnetic flux tubes 1 mm outside the separatrix with (blue) and without (red) kinetic correction. (b) Impurity radiation power integrated over the inner, outer, and the main SOL (above the X-point) with and without the kinetic correction.

values of the impurity density in the SOL are reduced by a factor of two. This is due to reduced thermal force by kinetic correction in a low-collisional region between the X-point and the inner and outer midplanes (Fig. 4 (a)). The impurity profiles near the divertor plates, where collisionality is high, are not affected by the kinetic correction (Fig. 4 (b)). Overall effects of the kinetic correction on total impurity radiation and the divertor heat load are about a few percent in the discharge condition analyzed. The kinetic correction is found to be more pronounced for higher-charge impurity states, due to charge dependence of the parallel impurity force balance. This indicates the importance of the effect for high-Z impurities such as tungsten in future devices.

(M. Kobayashi)

## Molecular Dynamics Simulation on Hydrogen Trapping on Tungsten Vacancy [5]

This study employs molecular dynamics to elucidate the influence of hydrogen on the structural transformation of vacancies in tungsten. The objective is to gain insight into the interaction between vacancies and hydrogen in tungsten. The simulations were performed at varying temperatures and with differing numbers of hydrogen atoms present within the vacancies. Figure 5 shows a snapshot of the atomic structure. The evaluation of four key parameters, namely the isopotential surface for the increase of total potential energy, the root mean square deviation of tungsten atoms, the root mean square fluctuation of tungsten atoms, and the density distribution in the radial direction, revealed that the presence of a substantial number of hydrogen atoms within a vacancy at each temperature resulted in notable alterations to the structural configuration. This finding supports the experimental observation that hydrogen retention activates the coalescence of two tungsten vacancies.

(H. Nakamura)

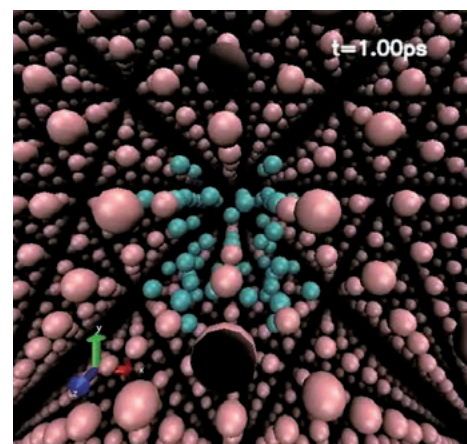


Fig. 5 Snapshot of the atomic structure at 1 ps simulation was performed by randomly injecting 54 hydrogen atoms into a vacancy created by the removal of 9 atoms from a tungsten bcc crystal. The blue and peach balls represent hydrogen and tungsten atoms, respectively.

## Enhanced Classical Radiation Damping of Electronic Cyclotron Motion in the Vicinity of the Van Hove Singularity in a Waveguide [6]

We study the damping process of electron cyclotron motion and the resulting emission in an electromagnetic rectangular waveguide, using the classical Friedrichs model without relying on perturbation analysis such as Fermi's golden rule. In this study, we consider the classical system where an electron inside the waveguide exhibits cyclotron motion with variable frequency under the influence of a (static, uniform) external magnetic field that is applied in parallel with the length of the waveguide (Fig. 6). A Van Hove singularity appears at the cutoff frequency of the dispersion associated with each of the electromagnetic field modes in the waveguide. In

the vicinity of the Van Hove singularity, we find that not only is the decay process associated with the resonance pole enhanced (amplification factor  $\sim 10^4$ ) but the branch-point effect is also comparably enhanced. As a result, the timescale on which most of the decay occurs is dramatically shortened. Further, this suggests that the non-Markovian branch-point effect should be experimentally observable in the vicinity of the Van Hove singularity. Our treatment yields a physically acceptable solution without the problematic runaway solution that is well known to appear in the traditional treatment of classical radiation damping, based on the Abraham–Lorentz equation.

(Y. Goto)

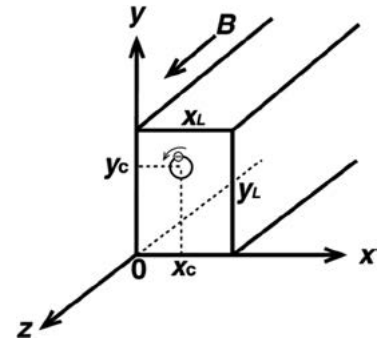


Fig. 6 Physical model and coordinate system.

## Theoretical and simulation studies of crescent-shaped ion velocity distributions in magnetic reconnection [7]

Crescent-shaped velocity distributions have been actively studied as one of the important issues related to magnetic reconnection. Crescent-shaped distributions have been observed by satellites in the Earth’s magnetosphere since the 1990s and analytical theories have recently been proposed. Consequently, it is believed by many researchers that magnetic-field reversal is necessary to the production of crescent distributions.

We, however, challenge the above accepted notion. We formulate a new theory which indicates that crescents are constructed under a uniform magnetic field alone. This implies that magnetic-field reversal is not required for crescents. Furthermore, according to our theory, three-dimensional crescents are formed by a combination of uniform and reversed components of the magnetic field. We carry out particle simulations of magnetic reconnection with a strong guide field. Figure 7 (a) shows the magnetic field lines and the guide magnetic field  $B_z$ , and Fig. 7 (b) displays velocity plots of ions in the boxed area of Fig. 7 (a). A three-dimensional crescent is clearly seen.

We expect that 3D crescent-shaped ion velocity distributions will be detected in the outflow region of magnetic reconnection with a guide magnetic field at the Earth’s magnetopause.

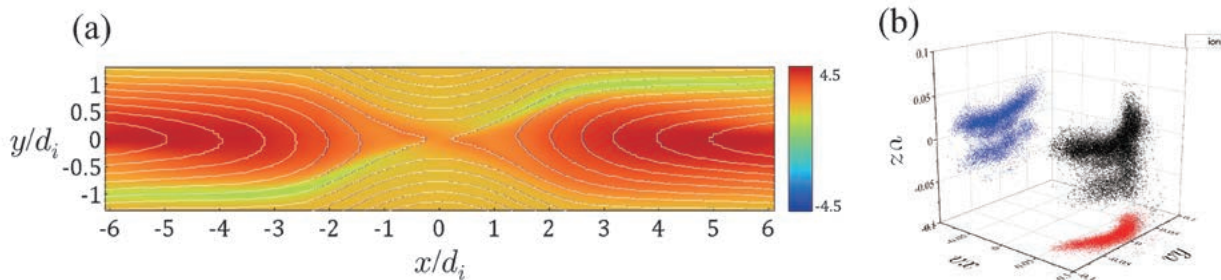


Fig. 7 (a) Magnetic field lines and  $B_z$  (color). Magnetic reconnection is driven in the center. (b) Velocity plots of ion particles as black points. We can see that the 3D structure of a crescent structure is formed in velocity space. Red and blue points are projections into the  $(v_x, v_y)$  and  $(v_y, v_z)$  planes, respectively.

(S. Usami)

- 
- [1] Mamoru Shoji *et al.*, “Simulation Analysis of Transport of Boron Dust Particles Injected by Impurity Powder Dropper in the Large Helical Device”, *J. Adv. Simlat. Sci. Eng.* **11**, pp. 12–20 (2024).
- [2] U. Wenzel, G. Motojima *et al.*, “Ultrahigh neutral pressures in the sub-divertor of the Large Helical Device”, *Nucl. Fusion* **64**, 034002 (2024).
- [3] M. Tokitani *et al.*, “Plasma Wall Interaction of New Type of Divertor Heat Removal Component in LHD Fabricated by Advanced Multi-Step Brazing (AMSB)”, *Fusion Sci. Technol.* **79**, pp. 651–661(2023).
- [4] M. Kobayashi *et al.*, “SOL impurity transport analysis with SONIC code with a kinetic effect on a thermal force transport model in JT-60U”, *Contrib. Plasma Phys.*, e202300141 (2024). <https://doi.org/10.1002/ctpp.202300141>
- [5] Hiroaki Nakamura *et al.*, “Molecular Dynamics Simulation on Hydrogen Trapping on Tungsten Vacancy”, *J. Adv. Simlat. Sci. Eng.* **10**, pp. 132–143 (2023). DOI: 10.15748/jasse.10.132.
- [6] Y. Goto *et al.*, “Enhanced Classical Radiation Damping of Electronic Cyclotron Motion in the Vicinity of the Van Hove Singularity in a Waveguide”, *Prog. Theor. Exp. Phys.*, 033A02 (2024).
- [7] S. Usami and S. Zenitani, *Phys. Plasmas* **31**, 022102 (2024).

# Sensing and Intellectualizing Technology Unit (S&I)

Observing, predicting, and controlling the behavior of ultra-high temperature plasma are essential subjects for improving the performance of fusion reactors. In S&I unit, we will develop dramatically high-precision plasma measurement methods and construct a system that enables holistic and precise plasma observation. Furthermore, we will analyze the data using data science and convert it into visual, auditory, tactile, and other information to make it “intellectualizable”. This effort, in which researchers specializing in measurement, data analysis, and expression methods work together to systematize the intellectual inquiry process, will revolutionize the understanding of phenomena in fusion science and many other scientific fields.

This chapter reports selected notable results from the S&I Unit in FY2023 related to plasma diagnostics, visualization, open science, isotope science, and other interdisciplinary research.

## Turbulence Transition in Magnetically Confined Hydrogen and Deuterium Plasmas

In toroidal devices, ion scale turbulence, of which wavelength is order of ion Larmor radius, plays a essential role for confinement. The ion scale turbulence changes its characteristics depending on plasma parameters and affects energy, particle and momentum transport. In LHD, we discovered turbulence transition from ion temperature gradient (ITG) to resistive interchange (RI) turbulence<sup>1</sup>. Figure 1 shows electron density dependence of turbulence level and phase velocity in laboratory frame. Turbulence level, which is normalized turbulence amplitude by local electron density and turbulence phase velocity were measured by the two-dimensional phase contrast imaging. In Fig. 1, the data was taken from the shot-by-shot basis density scan experiments under constant heating power with 1.4MW electron cyclotron resonant heating. Experiments were performed for hydrogen (H) and deuterium (D) plasma. As shown in Fig. 1 (a), turbulence level decreases to a transition density ( $n_{tr}$ ) and increase above it. Simultaneously, the propagation direction of turbulence phase velocity changes from ion diamagnetic direction to electron-diamagnetic direction. The turbulence level is almost comparable in H and D plasma under  $n_{tr}$  however, it is clearly lower in D plasma above it. Power balance analyses showed thermal conductivity driven by turbulence process scales with turbulence level and becomes minimum at  $n_{tr}$ . These results suggest that turbulence characteristics

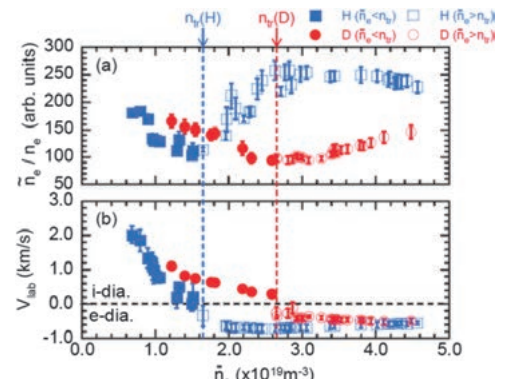


Fig. 1 The line averaged electron-density dependence of (a) the turbulence level and (b) phase velocity of turbulence in the laboratory frame.  $n_{tr}(H)$  and  $n_{tr}(D)$  represent the transition densities in the H and D plasmas, respectively. The blue and red symbols represent the H and D plasmas, respectively. The closed and open symbols represent  $\bar{n}_e < n_{tr}$  and  $\bar{n}_e > n_{tr}$ , respectively. The values are averaged at  $\rho = 0.5-0.7$

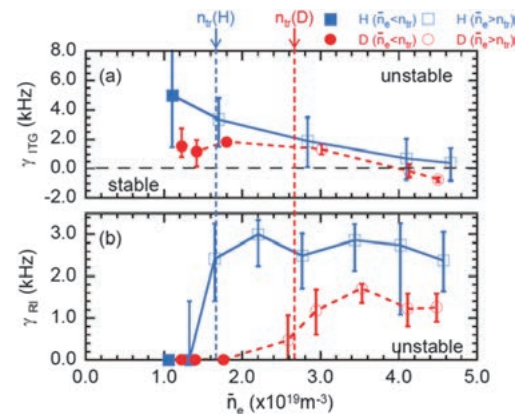


Fig. 2 Electron-density dependence of the linear growth rate of (a) ITG turbulence ( $\gamma_{ITG}$ ) and (b) RI turbulence ( $\gamma_{RI}$ ). The errors in  $\gamma_{ITG}$  and  $\gamma_{RI}$  were evaluated by changing the normalized ion temperature gradient and pressure gradient by 20 %, respectively.

changes at  $n_{tr}$ .

Then, theoretical investigation was performed. Firstly, gyro-kinetic linear analyses was done. Dominant instability was ITG turbulence in whole experimental regime. As shown in Fig. 2 (a), its growth rate ( $\gamma_{ITG}$ ) decrease with increase of density. This results qualitatively agree with observed density dependence at lower than  $n_{tr}$ , however, does not account at higher than  $n_{tr}$ . Then, we employed two-fluid MHD simulation. Figure 2 (b) shows density dependence of growth rate of RI turbulence ( $\gamma_{RI}$ ).  $\gamma_{RI}$  can not be evaluated by gyro-kinetic simulation, because of non-ballooning structure of Eigen function. RI can be unstable due the nature of magnetic hill in LHD. As shown in Fig. 2 (b),  $\gamma_{RI}$  becomes positive indicating RI is unstable above  $n_{tr}$ . Also,  $\gamma_{RI}$  is lower in D plasma at  $\bar{n}_e > n_{tr}$  and qualitatively account for the reduced turbulence level. At  $\bar{n}_e > n_{tr}$ , turbulence driven anomalous thermal conductivity is lower and global energy confinement time is higher in D plasma than H plasma. The reduced transport in D plasma at  $\bar{n}_e > n_{tr}$  is due to weaker RI turbulence. Weaker RI turbulence is due to the lower resistivity, heavier ion mass and lower pressure gradient due to the hollower density profile in D plasma.

[1] T. Kinoshita *et al.*, Physical Review Letters **132**, 235101 (2024).

(K. Tanaka and T. Kinoshita (Kyushu Univ.))

## New Parity Transition of Radial Structure of MHD Modes

The parity of the radial displacement profile of low-order MHD modes observed in magnetically confined plasmas is closely related to the topology of the magnetic field structure. The odd-parity structure typically reflects a large magnetic island structure, whereas the even-parity structure does a structure without an island. Thus, understanding parity transitions is key to elucidating the physical mechanisms of magnetic island formation and stabilization in magnetized plasmas such as fusion and astrophysical plasmas.

In tokamaks and the LHD, parity transitions from even to odd functions have been observed, providing circumstantial evidence of the contribution of even-parity MHD modes to magnetic island formation. Detailed mode structures have been obtained in the LHD using high-spatial-resolution interferometry, leading to the discovery of parity transitions from odd to even in addition to those from even to odd. This suggests that even-parity MHD modes also contribute to stabilizing magnetic islands, offering crucial new insights for developing predictive modeling for magnetic island formation and stabilization.

(Y. Takemura)

## Anomaly detection of radiative collapse using 2-D radiation measurement and imaging analysis

In the case of a divertor detachment using impurity injection to reduce the divertor heat load, increasing the amount of impurity injection can reduce the thermal load further, but if the injection amount is too much, radiative collapse occurs. Therefore, to control the amount of impurity injection and maintain the divertor detachment, it is necessary to detect the precursor of radiative collapse.

In multi-pulse neon (Ne) injected plasma in the LHD, by learning 1,086 images of 520 pixels measured by an

infrared imaging video bolometer using an autoencoder, the precursor was detected as an increase in abnormality before the Ne pulse that induced the radiative collapse.

(K. Mukai)

## Suppression of resistive interchange instability by external RMP

In the LHD, which is a heliotron type fusion device for the experiments, the resistive interchange MHD instabilities could disturb the stable and high discharges of the high beta plasma discharges. Then, the method to avoid and/or suppress the instabilities are being investigated. As our previous works [2], it is found that the imposing the RMP (resonant magnetic perturbation) by the external coils is effective to suppress the fluctuation due to the interchange instability. Here it should be noted that imposing the RMP field is also effective to suppress the MHD instabilities in the tokamaks. On the contrary, it is well known that the RMP field induces the strong degradation of the plasma confinement due to the magnetic island formation beyond a threshold of the RMP amplitude. Recently, we obtain the following empirical scaling law on the RMP amplitude to completely suppress the fluctuation due to the interchange instability through the LHD experiments with various plasma parameter regimes,

$$I_{RMP}/B_0 = 6.6 \times 10^2 \cdot \beta^{1.8} \cdot \nu^{*0.24} \cdot \rho^{*0.85}$$

Here  $I_{RMP}$ ,  $B_0$  are the coil current for the RMP and the operational magnetic field strength, respectively. And are the beta value, the normalized collisionality and gyro-radius at the rational surface. Moreover, the empirical scaling law on the RMP amplitude to degrade the confinement is obtained as follow,

$$I_{RMP}/B_0 = 4.9 \times 10^3 \cdot \beta^{1.3} \cdot \nu^{*-0.25} \cdot \rho^{*1.2}$$

From the above results, it is found that, in a heliotron type fusion device,  $(\beta, \nu^*, \rho^*) = (0.60\%, 4.2 \times 10^{-2}, 4.2 \times 10^{-4})$  [3], we could completely suppress the interchange MHD instability due to the imposing RMP externally without the strong degradation of the plasma confinement.

[2] S. Ito *et al.*, Nucl. Fusion **63**, 066016 (2023).

[3] T. Goto *et al.*, Nucl. Fusion **57**, 066011 (2017).

(K. Watanabe, Y. Takemura, S. Sakakibara,

S. Ito (Nagoya Univ.), H. Beniya (Nagoya Univ.) and S. Masamune (Chubu Univ.)

## Integrated virtual–reality visualization of simulation results and 3D model

Plasma, where various and complex phenomena take place, is one of the optimal subjects for applying visualization using virtual reality (VR) technologies. This paper reports the enhancement of the VR visualization software for the CAVE system, “VFIVE”. VFIVE is a general-purpose VR visualization software for the CAVE system, utilizing several visualization methods such as streamlines, arrows, isosurfaces, contour plots, and more. We have added three functions to VFIVE: 1) Streamlines from predefined starting points. 2) New streamline representations. 3) A fusion display of visualization results by VFIVE and the 3D model rendered by Unity. With

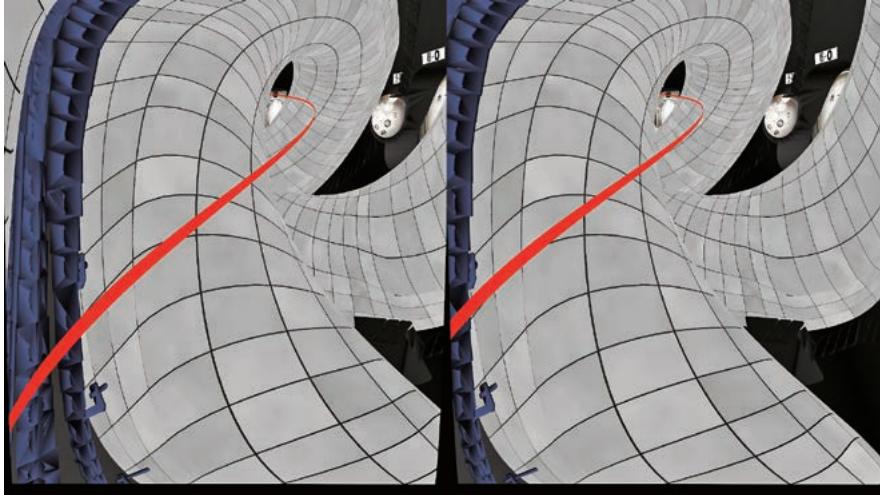


Fig. 3 Fusion visualization by VFIVE with libraries GLMetaseq and CLCL incorporated. Right and left figures are for right and left eyes, respectively.

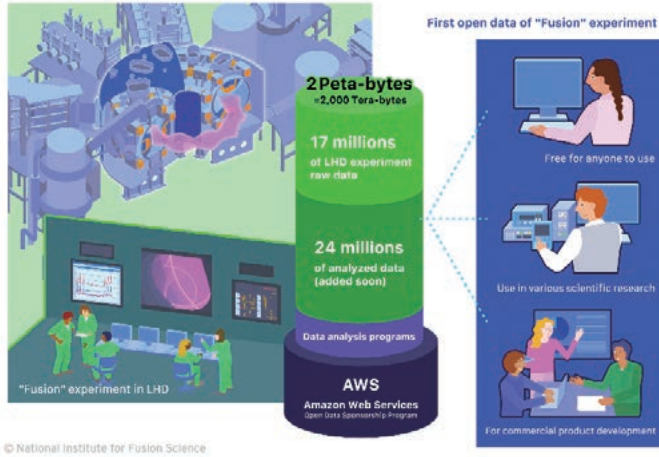
Function 1, we can estimate the backward streamlines from the starting points. Function 2 can show tube and ribbon representations in addition to the colored line, which is already implemented in VFIVE. Function 3 is realized by two methods: the commercial software “FusionSDK” by FiatLux and Cybernet on the CAVE system, and the GLMetaseq library on the head-mounted display system. The GLMetaseq library is a free library for C and C++, which reads MQO formatted 3D model data and displays it using OpenGL. MQO formatted data is generated by the free 3D modeling software, Metasequoia 4. In this process, after rendering by Unity is finished, Unity exports FBX formatted data. Metasequoia 4 imports the data and exports the old-style MQO formatted data. The figure shows a snapshot of the inside of the LHD vessel with tube streamlines by VFIVE, with the GLMetaseq and CLCL libraries incorporated. Visualizing simulation data within a device represented by a 3D model is expected to aid the observer’s intuitive understanding.

(H. Ohtani)

## 25 years of massive fusion energy experiment data completely open on the “cloud”, to be available to everyone

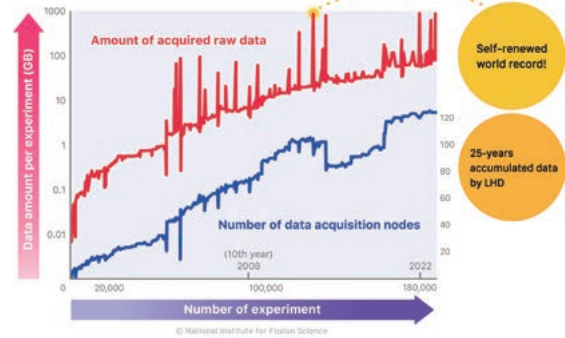
The National Institute for Fusion Science (NIFS) has been strongly promoting the “Open Data” in fusion research, and all the accumulated data through the past 25 years of operation of the Large Helical Device (LHD) fusion plasma experiments have been made fully open to the public on Amazon Web Services (AWS), with the support of the “AWS Open Data Sponsorship Program”.

To promote the use of large-scale experiment data, an important possibility exists in “cloud service” computer environment in which anyone can begin data analyses very quickly and easily. Therefore, about 17 million clusters of raw data (about 1.5 petabytes in archived size) acquired from LHD have been made freely available to the public on the same cloud storage, Amazon S3, since April 2024. An additional 24 million analytical results will be also open. (Figure 4) [4,5].



© National Institute for Fusion Science

Fig. 4 All diagnostic and analyzed data of LHD, having more than 40 million items and 2 petabytes in total, are open to the public on AWS’s cloud storage.



© National Institute for Fusion Science

Fig. 5 Amount of acquired raw data per LHD experiment (red line) and the number of diagnostic devices (blue line).

This is the first time in the world of fusion research that all experiment data have been made publicly open, making the newest research data available to anyone via the Internet. It is a major step toward making fusion energy research an “Open Science”. NIFS considers the fulfilment of the FAIR Principles, which is regarded as an important indicator toward Open Science, in diagnostic raw and analyzed data to be an important proposition of the “Academic Research Platform” LHD and continues its efforts. We also have started assigning DOIs (Digital Object Identifiers) to approximately 40 million LHD data to facilitate their findability and accessibility in accordance with the FAIR Principles.

The LHD diagnostic and analyzed data repository, which is the world’s largest accumulation of fusion energy research data, is a very valuable digital research asset. It is expected that the datasets will be used not only for research purposes within and outside fusion research but will also attract new entrants from citizens, industries and other countries that are interested in starting fusion energy research and development. Barriers for new entrants are expected to be significantly lowered. It will also serve as a major digital platform for research knowledge exchange, human exchange, and human development not only in Japan but also around the world. To this end, NIFS is intensively promoting this large-scale data repository under the name of the “**Plasma and Fusion Cloud**” by utilizing the NII RDC, the research data cloud infrastructure of the National Institute of Informatics (NII).

This research is supported by the Ministry of Education, Culture, Sports, Science and Technology (MEXT) under the contract with NII, which is implementing the “Research Data Ecosystem Development Project to Promote the Use of AIs” and has been selected as use case creation project No. 2023-6.

[4] AWS blog, <https://aws.amazon.com/jp/blogs/news/25years-huge-fusion-experiment-data-fully-open-on-s3-via-odp-2024/> (2024).

[5] NIFS press release, <https://www.nifs.ac.jp/news/collabo/240614.html> (2024).

(H. Nakanishi and M. Emoto)

## Analysis of molecular hydrogen (H<sub>2</sub>) in the atmosphere for understanding the behavior of atmospheric tritiated hydrogen (HT)

Tritium would be the fuel of the first-generation nuclear fusion reactor. Since it is radioactive material, the environmental monitoring of tritium would be required in the vicinity of the fusion facility site from the viewpoints of radiation safety and public acceptance. As one of the environmental tritium monitoring items, atmospheric tritium measurement is important. Tritium in the atmosphere has three chemical forms: tritiated water vapor (HTO), tritiated molecular hydrogen (HT), and tritiated methane (CH<sub>3</sub>T). The atmospheric tritium monitoring system with different chemical forms has been developed and operated at the NIFS Toki site since 2004 [6]. The tritium monitoring results indicated that the specific activity of HT and CH<sub>3</sub>T is much higher than that of HTO [7]. To investigate the cause of high specific activity, we focus on the behavior of molecular hydrogen (H<sub>2</sub>) in the atmosphere and develop a continuous measurement system based on a gas chromatograph and trace reduction detector. Monitoring results showed that the range of the H<sub>2</sub> mixing ratio at the NIFS Toki site was 0.4~0.6 ppm over the observation period. Atmospheric H<sub>2</sub> concentrations were higher during the daytime and long daylight seasons such as summer, suggesting the generation of hydrogen by photochemical reactions. Preliminary results suggest that there does not appear to be a clear correlation between the concentration of atmospheric HT and the concentration of H<sub>2</sub> in the atmosphere. This suggests that the source of HT is different from the source of H<sub>2</sub> in the atmosphere. For future studies, long-term observational data of both HT and H<sub>2</sub> and the seasonal variation of HT in the wide latitude range with a joint research project are needed to obtain clear conclusions [8].

[6] T. Uda *et al.*, *Fusion Engineering and Design* **81**, 1385–1390 (2006).

[7] M. Tanaka and T. Uda, *Radiation Protection Dosimetry* **167**, 187–191 (2015).

[8] M. Tanaka *et al.*, *Plasma and Fusion Research* **18**, 2405038 (2023).

(M. Tanaka)

## Femtosecond Optical Vortex Laser Processing for Fusion Materials

We have research about laser processing for fusion materials employing optical vortex laser to improve the material properties and processing efficiency. In the FY2023 research, we investigated femtosecond vector vortex laser processing for tungsten including laser-induced periodic surface structure (LIPSS) formation. Optical vortex laser processing showed an ablation threshold three times higher than that of conventional Gaussian beams (Fig. 6 (a)). Furthermore, the vector vortex laser with controllable the structured two-dimensional spatial distribution of polarization realized fabrication of the complex LIPSS pattern like a helical surface relief (Fig. 6 (b)). Femtosecond vector vortex laser processing would provide us with robust and flexible surface processing method, and open the door to innovative applications of tungsten materials.

This research is the collaboration project between NIFS, the RIKEN (Dr. Sugioka) and the Nagoya Institute of Technology (Dr. Miyagawa), and these results were published in the academic journal of “Optical Material Express” (IF: 2.8) published by Optica Publishing Group (USA).

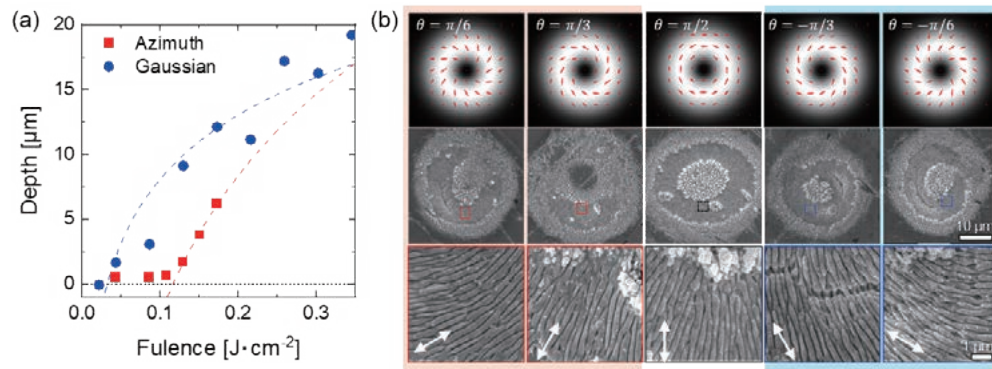


Fig. 6 (a) Dependence of ablation depth  $D$  on laser fluence in the laser irradiation to tungsten surface, (b) Fabricated chiral surface structures employing vector vortex laser. by H. Kawaguchi. (Figure adapted from “Opt. Mater. Express **14**, 424–434, 2024”)

(H. Kawaguchi, R. Miyagawa (NITech, NIFS) and K. Sugioka (RIKEN))

# Plasma Apparatus Unit

A plasma apparatus (PA) unit, as an axis of plasma science and technology, started in the fiscal year 2023 when a system of units started at NIFS. The importance of disruptive innovation as a game changer in fusion research has been pointed out. To this end, The PA unit will aspire to create innovative plasma technology by deepening scientific knowledge of the complex collective phenomena of plasma. By developing novel applications of plasma as working hypotheses, the PA unit will promote collaboration in fusion with other fields and shed light on the unexplored emergent nature of collective phenomena. The innovation of plasma science and technology will open a new horizon for various natural sciences research and science and technologies.

Toward the above end, four research topics have started in the PA unit: the neutral beam injector, anti-material and dipole plasma, muon science, and electric propulsion.

## Neutral Beam Injector

A radio frequency (RF) negative ion source was applied to the Neutral Beam Injector (NBI) for ITER. One of the targets to be achieved is a smaller beam divergence than 7 mrad, which has been achieved by a filament-driven arc (FA) negative ion source for the NBI in the Large Helical Device at NIFS. It has not been clarified why the beam divergence of the RF negative source is larger than that of the FA. To compare the beam divergences of the FA and RF sources with the same diagnostics at the same ion source directly, and to investigate the physics mechanism of the beam divergence difference, collaborating with the ITER Organization (IO) and the Max-Planck Institute for Plasma Science (IPP, Germany), an FA/RF hybrid negative ion source has been developed, based on research and development of an FA negative ion source (NIFS-RNIS). The FA/RF hybrid negative ion source operations, which are only FA or RF and FA/RF hybrid discharges and beam extraction, have been accomplished [1]. Following this achievement, an international joint collaboration experiment with NIFS, IO, IPP, the National Institutes for Quantum Science and Technology, Consorzio RFX (Italy), the High Energy Accelerator Research Organization (KEK), and Doshisha University was performed for a month. The FA and RF ion source plasmas had almost the same profiles in the direction of the magnetic filter. The plasma potential in the RF ion source plasma was several times higher than that in the FA. The collaboration with KEK brought the possibility of oscillating the beam divergence by the oscillation of plasma production [Shibata]. An international collaboration, including domestic institutes in not only the fusion field but also other fields, such as the accelerator science, and collaboration with academic and development institutes will find solutions to the NBI tasks and can open new frontiers in science and technology.

[1] H. Nakano *et al.*, 29th IAEA Fusion Energy Conference (2023); K. Tsumori *et al.*, 20th International Conference on Ion Sources (2023).

[2] T. Shibata *et al.*, J. Phys.: Conf. Ser. 2743, 012007 (2024).

## Anti-Material Plasma and Dipole Plasma

The levitated dipole configuration is globally analogous to planetary magnetospheres and is capable of confining high-beta plasmas suitable for an advanced fusion concept. Phenomena in fusion-oriented plasmas and geospaces share commonalities in terms of waves and transport properties. Moreover, the excellent confinement

properties of a levitated dipole enable new experiments such as antimatter plasmas. We are conducting interdisciplinary studies in the dipole magnetic field configuration, focusing on the creation and understanding of electron-positron plasmas and laboratory studies on wave phenomena in geospace. Regarding electron-positron plasmas, by utilizing a linac-based pulsed positron source, we have captured 105 positrons in the dipole magnetic field, which is over 100 times the previous record. Although the captured positron cloud still does not satisfy the plasma condition, we are developing a strong magnetic field trap to accumulate up to 109 positrons in a steady magnetic field of 5 T over a 60 cm region in the axial direction. As well as a pure electron plasma experiment in this trap, we are conducting the construction of a compact levitated dipole for the confinement of positrons with electrons as pair plasmas. On plasma wave experiments, we have conducted laboratory studies on whistler-mode chorus emissions in RT-1, as a collaboration work between the Plasma Apparatus Unit and the Phase Space Turbulence Unit. By adjusting the ratio of hot-electron components in the plasma, we have demonstrated the spontaneous generation of chirping chorus emissions and investigated their appearance conditions. Through these experiments, we have shown that the presence of a simple dipole magnetic field and hot electrons are the conditions that drive chorus emissions, indicating that this is a universal phenomenon in both celestial bodies and laboratories [1].

[1] H. Saito *et al.*, *Nature Communications* **15**, 861 (2024).

## Muon Science

The following reports the advancements in muon science achieved in 2023. Two major achievements were made using superconducting X-ray detectors with excellent energy resolution. Firstly, notable advancements were made in the high-precision X-ray spectroscopy of muonic atoms. This research involved measuring the transition energies of muonic atoms, where a muon replaces an electron, creating an environment with extremely strong electric fields between the muon and the atomic nucleus. This allowed for the verification of quantum electrodynamics (QED) under such intense conditions. The results were published in *Physical Review Letters* [1] (PRL130, 173001(2023)).

Secondly, groundbreaking work was accomplished with the first successful global application of high-resolution X-ray spectroscopy on the dissociation of resonant states in muonic molecules. This breakthrough helps elucidate the complex quantum mechanical dynamics involved in the muon-catalyzed fusion ( $\mu$ CF) process. These findings contribute significantly to the theoretical and practical understanding of  $\mu$ CF, which is essential for future applications.

[1] T. Okumura *et al.*, *Phys. Rev. Lett.* **130**, 173001 (2023).

## Electric Propulsion

Fundamental studies on plasma dynamics relating to plasma production and expansion in a magnetic nozzle configuration are done via laboratory experiments. These insights are applied to an electric propulsion device in space and industrial plasma devices, e.g., plasma etching [2]. Assessment of the performance of the magnetic nozzle radio frequency plasma thruster has shown its efficiency approaching 30 percent, which is the highest to date. The key issue for the performance improvement seems to be the inhibition of the energy loss to the radial source boundary, which can be achieved with the help of a magnetically-confined fusion plasma community, where a cusp magnetic field is applied in the source tube [1]. Toward further development of an engineering model of the thruster, a permanent magnet configuration is designed to form the cusp, where the source is contiguously attached to a diffusion chamber, showing an increase in the plasma density in the magnetic nozzle region [3]. As a new type of compact electric propulsion device, a water-fueled magnetron sputtering thruster is proposed and investigated, showing the thrust generation by the sputtered materials. Since the sputtered atoms are electrically neutral, the momentum ejection from the system can be achieved with no neutralizer, providing a very compact and simple propulsion system [7]. The research on the magnetic nozzle rf plasma thruster is now extended to an international collaboration between Tohoku University and Deutsches Zentrum fuer Luft- und Raumfahrt (DLR). Furthermore, the development of the plasma etching device has been progressed over the last few years.

- [1] K. Takahashi, *J. Phys. D: Applied Phys.* **56**, 475207 (2023).
- [2] K. Takahashi *et al.*, *Plasma and Fusion Res.* **18**, 2501050 (2023).
- [3] Y. Nakahama and K. Takahashi, *AIP Advances* **14**, 015059 (2024).
- [4] K. Takahashi, *J. Plasma Phys.* **90**, 975900201 (2024).
- [5] S. Sumikawa and K. Takahashi, *Phys. Plasmas* **31**, 034501 (2024).
- [6] K. Takahashi and S. Sumikawa, *Plasma Phys. Contr. Fusion* **66**, 015012 (2024).
- [7] S. Shimizu and K. Takahashi, *J. Plasma Phys.* **90**, 975900205 (2024).

(H. Nakano<sup>1</sup>, H. Saito<sup>1,2</sup>, S. Okada<sup>1,3</sup> and K. Takahashi<sup>4</sup> (<sup>1</sup>NIFS, <sup>2</sup>Univ. Tokyo, <sup>3</sup>Chubu Univ., <sup>4</sup>Tohoku Univ.))

# Complex Global Simulation Unit

In order to understand the behavior of an entire system composed of multiple hierarchies, individual simulations of each hierarchy are not sufficient. Global simulations that consider the interactions between hierarchies are required. Such complex global simulations are an important issue that is expected to be realized not only in the field of nuclear fusion research (Fig. 1) but also in many other academic fields. However, their realization is not easy. The reason for this is that the temporal and spatial scales of a microscopic hierarchy and the entire system are often extremely different, and the capacity and capability of the computer are not sufficient to simulate the entire range of scales based on a single system of fundamental physical equations. The purpose of this unit is to develop simulation methods to solve this problem and to promote simulation research.

The Complex Global Simulation Unit aims to develop simulation methods that couple different hierarchies and physical models to realize global simulations that predict and elucidate the behavior of entire physical systems that cannot be handled by simulations based on a single system of fundamental physical equations. This unit will develop 1) global simulations of the whole of a magnetic confinement fusion plasma, including core and edge plasmas, based on kinetic-magnetohydrodynamic hybrid simulation, and 2) a methodology with broad applicability to achieve simulations that more closely reproduces real-world phenomena, beyond the severe limitations imposed by the capacity and capability of supercomputers. To develop such simulation methods, we must enhance our understanding of the physics of each different hierarchy and the interactions between them. The development of advanced theories is also crucial. Our recent studies have yielded successful results in 2023-2024, as shown in the following pages.

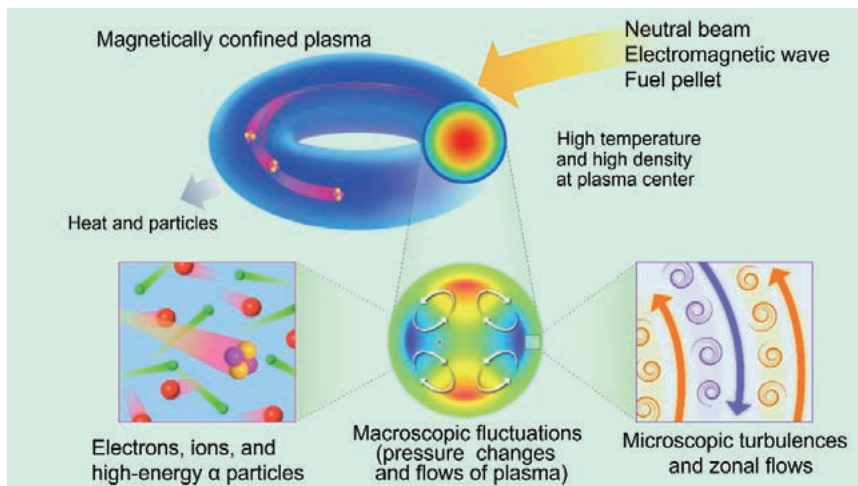


Fig. 1 Multiple hierarchies of a burning fusion plasma

(M. Toida)

## Kinetic-MHD hybrid simulation of infernal modes in tokamak plasmas

For realizing a steady-state fusion reactor, high-beta plasma must be stably confined for a long time. In high-beta plasmas, non-inductive bootstrap current becomes large, and discharges with an increased proportion of bootstrap current are one of the steady-state operation scenarios in tokamak plasmas. For such plasmas, since magnetic shear is weak in the core region, infernal modes driven by the pressure gradient are considered to limit the poloidal-beta value in tokamak plasmas. Therefore, suppression of the infernal mode is one of the key

issues in plasma discharges with large bootstrap currents in tokamaks. In this study, the influence of the infernal modes on the plasma confinement is investigated by simulations [1]. The simulations are performed using the MIPS code based on the MHD model and the MEGA code based on the kinetic-MHD hybrid model with kinetic thermal ions (KTIs).

Figure 2 shows the time evolution of a pressure profile on a poloidal cross-section obtained from simulations for a resistive infernal mode. In the MHD simulation without KTIs, the pressure profile is significantly deformed, which causes a significant decrease in the beta value. On the other hand, in the kinetic-MHD hybrid simulation with KTIs, deformation of the pressure profile is significantly suppressed, and the decrease of the beta value is very small, almost maintaining its initial value. This indicates that kinetic thermal ions play an essential role in suppressing the flattening of the pressure profile due to slowly growing resistive MHD instabilities.

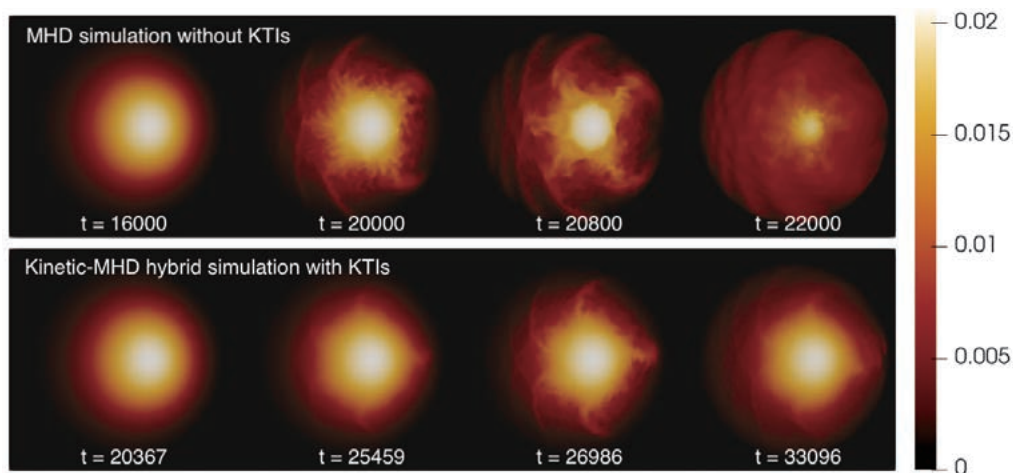


Fig. 2 Time evolution of the pressure profile on a poloidal cross section obtained from the MHD simulation without KTIs (the upper row) and the kinetic-MHD hybrid simulation with KTIs (the lower row) for a resistive infernal mode. Time is normalized by Alfvén time.

[1] M. Sato, Y. Todo, N. Aiba and M. Takechi, *Nuclear Fusion* **64**, 076021 (2024).

(M. Sato)

## Local momentum balance in electromagnetic gyrokinetic systems

Gyrokinetics is a powerful theoretical framework based on which a large number of analytical and numerical studies on microinstabilities and turbulent processes in magnetized plasmas have been done. The Eulerian variational formulation is presented to obtain governing equations of the electromagnetic turbulent gyrokinetic system. A local momentum balance in the system is derived [2] from the invariance of the Lagrangian of the system under an arbitrary spatial coordinate transformation, by extending the previous work [3]. The gyrokinetic Poisson equation and Ampère's law, derived from the variational principle, correctly describe polarization and magnetization due to finite gyroradii and electromagnetic microturbulence. Also shown is how the momentum balance is influenced by including collisions and external sources. Momentum transport due to collisions and turbulence is represented by a symmetric pressure tensor, which originates in a variational derivative of the Lagrangian with respect to the metric tensor. The relations of the axisymmetry and quasi-axisymmetry of the toroidal background magnetic field to a

conservation form of the local momentum-balance equation are clarified. In addition, an ensemble-averaged total momentum-balance equation is shown to take the conservation form, even in a background field with no symmetry, when a constraint condition representing the macroscopic Ampère’s law is imposed on the background field. Using the WKB representation, the ensemble-averaged pressure tensor due to the microturbulence is expressed in detail and verified to reproduce the toroidal-momentum transport derived in previous works for axisymmetric systems. The local momentum-balance equation and the pressure tensor obtained in this work are helpful references for elaborate gyrokinetic simulation studies of momentum- transport processes.

$$\frac{\partial}{\partial t} \left( \sum_a \int d^3v F_a \mathbf{p}_a \right) - \sum_a \int d^3v \mathcal{K}_a \mathbf{p}_a + \nabla \cdot \Theta = (\nabla \mathbf{A}) \cdot \frac{\delta L_{GKF}}{\delta \mathbf{A}} - \nabla \cdot \left( \frac{\delta L_{GKF}}{\delta \mathbf{A}} \mathbf{A} \right)$$

$$\Theta^{ij} \equiv 2 \frac{\delta L_{GKF}}{\delta g_{ij}}$$

Fig. 3 The local momentum-balance equation (upper) and the symmetric-pressure tensor derived from the variational derivative of the Lagrangian with respect to the metric tensor (lower).

- [2] H. Sugama, Phys. Plasmas **31**, 042303 (2024).
- [3] H. Sugama et al., Phys. Plasmas **28**, 022312 (2021).

(H. Sugama)

## Harmonic structure of lower hybrid waves driven by ring-like energetic ions

Energetic ions with a ring-like distribution in velocity space perpendicular to a magnetic field are produced through various processes, such as neutral beam injection, magnetic reconnection, and particle acceleration by a shock wave. The ring-like energetic ions can drive lower-hybrid wave (LHW) instabilities. Recently, harmonic LHWs have been observed in a fusion plasma and the Earth’s magnetosphere. We have studied the excitation mechanism of the harmonic LHWs through electromagnetic particle-in-cell simulations, considering the effects of the energetic-ion injection. It has been found that after the LHWs are excited with the wavenumber and frequency of  $(k, \omega)$ , many harmonic LHWs are generated at  $(mk, n\omega)$ , where  $m$  and  $n$  are integers, due to nonlinear wave-wave coupling, as shown in Fig. 4 [4].

In addition, motivated by satellite observations of the harmonic LHWs in the Earth’s polar region, we have per-

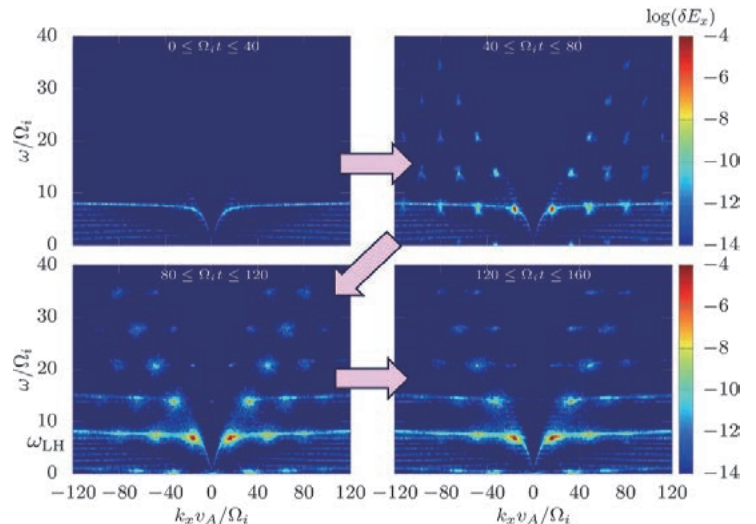


Fig. 4 Evolution of power spectrum of electric field fluctuations excited by ring-like energetic ions. The harmonic structure of LHWs is created due to nonlinear wave-wave coupling.

formed simulations by setting parameter values for the observations. The results show that the energetic ions can generate the harmonic LHWs, and background ions are more strongly accelerated when harmonics with large amplitudes are created [5]. This reveals the possibility that harmonic LHWs are involved in ion-acceleration phenomena commonly observed in the polar region, which has been an unsolved problem.

The numerical simulations were performed on the Plasma Simulator of NIFS.

[4] T. Kotani, M. Toida, T. Moritaka, and S. Taguchi, *Physical Review E* **108**, 035208 (2023).

[5] T. Kotani, M. Toida, T. Moritaka, and S. Taguchi, *Geophysical Research Letters* **50**, e2022GL102356 (2023).

(M. Toida)

## Non-ideal MHD growth of current interchange tearing modes at plasma edge and response to externally-imposed flow

A response of current interchange tearing modes (CITMs) to two-fluid and gyro-viscous effects is numerically studied. The CITM represents a transition phenomenon from the interchange to the tearing mode by current transport outside a last-closed flux surface (LCFS). The CITM has been proposed to explain an intermittent current eruption in the tokamak edge region. Two-dimensional numerical simulations are performed together with an effect of the current transport, modeled as a diffusive process. In a simulation without the diffusive model, the interchange modes grow as shown in the upper panel of Fig. 5. The growth of CITMs outside the LCFS is observed by applying the diffusive transport model in a single-fluid MHD simulation (middle panel) and an extended MHD simulation with a two-fluid and gyro-viscous model (bottom panel). These simulations show that the growth of CITMs significantly suppresses the deformation of magnetic field lines. A response of the CITMs to an externally imposed flow is also studied. The growth of a CITM is observed for a relatively small flow velocity (whether a flow is externally imposed or not), resulting in a suppression of the electric current outside the LCFS. It is also found that a columnar or stripe pattern is formed during CITM growth.

The numerical simulations were performed on the Plasma Simulator of NIFS, Oakforest-PACS (FUJITSU) of the JCAHPC, and Wisteria/BDEC-01 Odyssey (FUJITSU FX1000) of the University of Tokyo.

[6] Hideaki Miura, Linjin Zheng, and Wendell Horton, “Non-ideal MHD growth of current interchange tearing modes at plasma edge and response to externally-imposed flow”, *Physics of Plasmas* **30**, 052503 (2023).

(H. Miura)

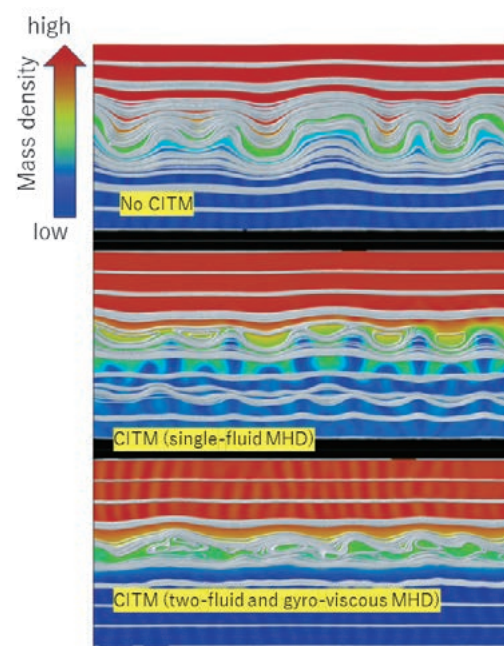


Fig. 5 Mass density (color contours) and 2D magnetic field lines in simulations in which CITM is not observed (top), CITM is observed in a single-fluid MHD simulation (middle), and CITM is deformed by two-fluid and gyro-viscous effects (bottom).

# Ultrahigh-flux Concentering Materials Unit (UlCoMat)

## Highlight

### Effects of annealing temperature on microstructure and hardness changes of cold rolled high-purity vanadium alloys

Low-activation vanadium alloy, V-4Cr-4Ti, is considered a candidate structural material for blanket applications in fusion reactors. High-purity vanadium alloys containing much lower levels of high-activation impurities (Co, Ni, Nb, Mo etc.) and interstitial impurities (C, N, O) have been developed to enhance low-activation characteristics and reduce cooling periods after use in fusion reactors. Moreover, decreasing the Ti concentration enables further improvement of the low-activation property, thus shortening the recycling periods. To clarify the recrystallization behavior of the high-purity vanadium alloys with different Ti concentrations (up to 4 wt%), the microstructure and hardness changes of the cold rolled vanadium alloys after 873–1273 K annealing were investigated [1]. As shown in Fig. 1, recovery and recrystallization took place while increasing the annealing temperature. Partial recrystallization occurred at 1073 K, and recrystallization finished at 1273 K. The size of the recrystallized grains decreased with the Ti addition. Precipitation was not observed in V-4Cr-0Ti, whereas Ti(CON) particles were formed in Ti-added alloys, V-4Cr-(1~4)Ti, after annealing at 973 K and above. The particle size rose together with an increasing Ti concentration and annealing temperature. The hardness of cold rolled vanadium alloys decreased while increasing the annealing temperature up to 1173 K, which was attributed to recovery of dislocations and the recrystallization process. The hardness increased with the higher Ti concentration, indicating solid-solution hardening via Ti. Additionally, further reducing high-activation impurities and interstitial impurities did not have significant impacts on the hardness of the V-4Cr-4Ti alloy after recrystallization.

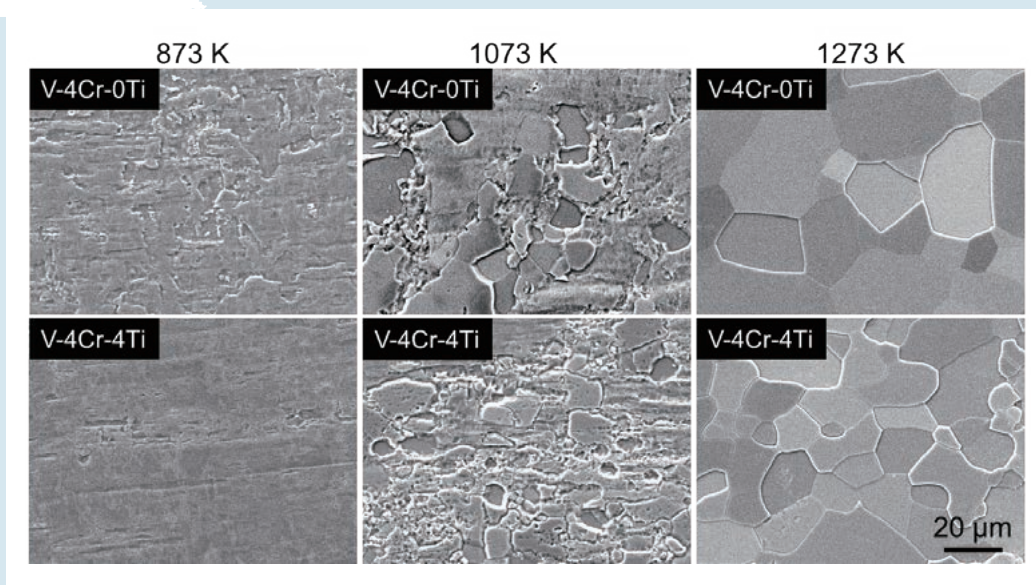


Fig. 1 Scanning electron microscope (SEM) images of cold rolled high-purity vanadium alloys after 873–1273 K annealing for 1 h.

(J.J. Shen)

## Recycling of low-activation vanadium alloys within ten years after use in fusion reactors

A contact dose rate of an existing V-4Cr-4Ti alloy, NIFS-HEAT-2, aligns at a remote-material-recycling level of  $10^{-2}$  Sv/h after a radioactivity cooling of 26 years. The present study proposes much earlier material recycling, typically within ten years, leading to an extreme reduction in the volume of radioactive material storage, and reuse in the same fusion reactor because ten years are sufficiently shorter than the reactor lifespan, about 30 years. These measures accelerate innovations for economic efficiency, safety and the social acceptance of fusion reactors. Material R&D essentials are (1) purification focusing on the high-activation impurities, such as Co, Cu, Fe, Nb, Ni and Mo, (2) minimization of the Ti concentration to avoid nuclear reactions from  $^{48}\text{Ti}$  to high-activation  $^{42}\text{K}$ , (3) removal of  $^{42}\text{Ar}$ , the long-lived mother for  $^{42}\text{K}$ . (1) Purification has been examined by aqueous-solution refining for  $\text{NH}_4\text{VO}_3$  as the precursor of vanadium metal, subsequent electron-beam refining and zone refining. The impurity levels achieved were 0.01 mass ppm for Co, <0.05 for Cu, 0.12 for Fe, 0.86 for Nb, 0.03 for Ni, and 10 for Mo [2]. They successfully satisfied the ten-year remote-recycling level. The vaporization coefficient at the gas-liquid interface in vacuum melting, and the segregation coefficient at the liquid-solid interface in zone refining were likely better for removal of Co from V, compared with Co from steels. Quantitative measurements of the coefficients are ongoing.

(T. Nagasaka)

## Applicability study on photoluminescence properties of $\text{Er}_2\text{O}_3$ for irradiation damage and temperature monitoring in fusion reactors

In photoluminescence (PL) spectra of  $\text{Er}_2\text{O}_3$  materials excited by an ultraviolet LED light source (365 nm), luminescence peaks were observed in the green (510–590 nm) and red (630–725 nm) ranges. Changes in the intensities of these luminescence peaks were examined for a commercially available sintered  $\text{Er}_2\text{O}_3$  disc and  $\text{Er}_2\text{O}_3$  powders fabricated with lower crystallinities. The results showed that the intensities of the red luminescence peaks decreased drastically compared with those of the green ones in  $\text{Er}_2\text{O}_3$  powders with lower crystallinities. Since the crystallinities of materials irradiated with neutrons degrade due to irradiation damage, this property could be used for irradiation damage monitoring of materials in fusion reactors. Changes in the intensities of the luminescence peaks with temperature were also examined for a sintered  $\text{Er}_2\text{O}_3$  disc. From room temperature to  $\sim 400$  °C, the intensities of the green luminescence peaks decreased drastically compared with those of the red ones.  $\text{Er}_2\text{O}_3$  materials could also be used for temperature monitoring in fusion reactors by using the property. It would be possible to perform the irradiation damage and temperature monitoring in fusion reactors during maintenance periods by using optical fibers, lenses, light sources and spectrometers [3]. The influence of induced gamma-rays emitted from radioactivated in-vessel components on the optical monitoring system is being investigated.

(T. Tanaka)

## One-step fabrication of $\text{Li}_2\text{TiO}_3$ ceramic pebbles using pulsed YAG laser

In a fusion demonstration reactor, a large amount of Li-containing ceramic breeder pebbles will be packed in a solid breeding blanket. Several pebble fabrication technologies have been proposed in previous studies, including the wet process, the emulsion method, extrusion spheronization, additive manufacturing, and the melt process. However, a simple, energy-effective, and scalable fabrication technology remains to be developed for the automated mass production and reprocessing of used radioactive pebbles post-operation. Selective laser melting potentially enables the quick and automated fabrication of breeder pebbles. Herein, we employ a high-power density pulse laser to produce ceramic breeder pebbles [4]. A pulsed YAG laser was irradiated over a lithium metatitanate ( $\text{Li}_2\text{TiO}_3$ ) powder bed in air, and the corresponding temperature was monitored using fiber-type infrared pyrometers. Spherical  $\text{Li}_2\text{TiO}_3$  pebbles were successfully fabricated in a single step with an average diameter of  $0.78\ \mu\text{m}$  and a sintering density of 87.4% (input power: 7.9 J/pulse). The irradiated  $\text{Li}_2\text{TiO}_3$  powder melted and turned spherical under surface tension and rapidly solidified, resulting in uniaxial fine grains and a decrease in the degree of long-range cation ordering.

(K. Mukai)

## Simultaneous measurements method for fast-neutron flux and tritium-production rate using single crystal CVD diamond detector

The breeding blanket (BB) systems of a Deuterium-Tritium (D-T) fusion reactor have been designed using advanced and updated nuclear data libraries, although uncertainties in these calculations would impact on the BB performance such as the tritium breeding ratio. Therefore, the present study developed a simultaneous measurement method for fast neutron energy spectra and the tritium production rate, using a single crystal Chemical Vapor Deposition (CVD) diamond detector (SDD), combined with a lithium fluoride (LiF) foil, applicable for BB performance evaluation.

14 MeV neutron irradiation was carried out on the SDD [5]. Fast neutrons could be detected by the SDD through elastic collisions and  $(n,\alpha)$  reactions, besides energetic tritons, produced in the LiF through the reaction with neutrons, could deposit the recoil energy into the SDD to be detected. We developed a code to separate pulses induced by fast neutrons and energetic tritons based on the shape, width, and height of pulses in the SDD, rejecting those induced by gamma-rays simultaneously. Subsequently, the fast neutron energy spectrum and tritium production rate were successfully deduced from discriminated-pulse data, using the response-matrix method and particle transport calculations.

(M. Kobayashi)

[1] J.J. Shen *et al.*, *Fusion Engineering and Design* **194**, 113905 (2023).

[2] T. Nagasaka *et al.*, *Materials Science Forum* **1106**, 117–126 (2023).

[3] T. Tanaka *et al.*, *Nuclear Materials and Energy* **38**, 101614 (2024).

[4] K. Mukai *et al.*, *Journal of the American Ceramic Society* **106**, 5735–5742 (2023).

[5] M.I. Kobayashi *et al.*, *Nuclear Fusion* **64**, 066026, (2024).

# Applied Superconductivity and Cryogenics Unit (ASC)

## Highlight

### FY2023 Research Results in the Applied Superconductivity and Cryogenics Unit

We have conducted thermal runaway tests in liquid hydrogen for REBCO, and have demonstrated that “cooling-stable” conditions, in which a transition to normal conduction does not lead to thermal runaway, can be met even with liquid hydrogen cooling.

We used a method (rotary magnetization) for a non-destructive, non-contact inspection of areas of  $I_c$  degradation in conductors made of laminated high-temperature superconducting wires, to measure magnetization signals and perform analysis using the finite element method. We demonstrated that it is possible to grasp the depth of deteriorated areas by changes in the magnetization-signal strength.

We developed a deep learning model to predict the ambient temperature of LHD helical coils based on measurement data accumulated during the LHD operation. We succeeded in highly accurate prediction of temperature changes that occur when helical coils are excited.

We succeeded in making an ultra-fine wire with a diameter of 50  $\mu\text{m}$  using Nb<sub>3</sub>Al wire, and succeeded in making a long single wire of significantly more than 6,000 meters without breakage or abnormal deformation during processing.

We are proceeding with the development of a practical 20 kA class STARS conductor, which is a simple laminate of REBCO wire, and conducted a second cooling and excitation test on a test sample with a 600 mm diameter, a three-turn solenoid coil shape and demonstrated stable current-carrying characteristics in high-speed excitation tests up to 200 times.

#### Keywords:

Advanced superconducting conductor  
Large scale superconducting coil  
Ultra-fine superconducting wire processing  
Liquid hydrogen  
AI predictive maintenance  
Machine learning  
SDGs (power saving)  
Carbon neutral

(N. Hirano)

## Introduction of Machine Learning to Superconducting and Cryogenic Systems

To improve the reliability of large-scale superconducting magnet and cryogenic systems, we have been developing a system incorporating machine-learning technology. NIFS has accumulated big data on superconducting magnets and cryogenic equipment through the operation of the LHD and experiments using cryogenic test facilities. It is possible to advance system development based on these big data. The aims of system development are status monitoring and virtual measurement. In the development, the target devices are core equipment of the superconducting magnet and cryogenic systems, as shown in Fig. 1. Regarding system-status monitoring, we use principal-component analysis, which is a machine-learning technique, to reduce the dimensionality of the measurement parameters used in the system. Furthermore, we use deep learning to centralize the measurement parameters. This dimensionality reduction and centralization will simplify the system-status monitoring. Regarding the system's virtual measurement, we use soft sensors simulating the measurement sensors used in actual measurements to provide sensor redundancy. This enables the system to operate normally, even if a problem occurs with the measurement sensor.

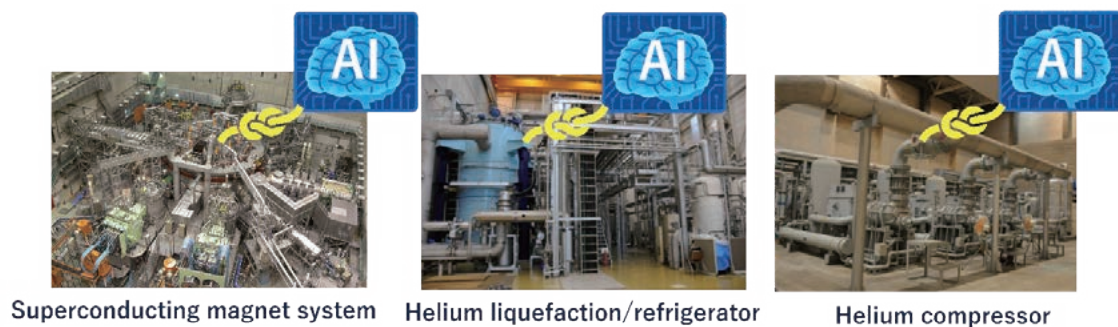


Fig. 1 Superconducting magnet and cryogenic systems with machine-learning technology.

(T. Obana)

## Development of High-Temperature-Superconducting Large-Current Conductor

The High-Temperature Superconducting (HTS) magnet may become a feasible option for fusion reactors. Using HTS conductors and high cryogenic stability at an elevated temperature, the operation is expected not to consume much helium. At the National Institute for Fusion Science (NIFS), three types of large-current HTS conductors have been developed, namely, the STARS, FAIR, and WISE conductors. The STARS (Stacked Tapes Assembled in Rigid Structure) has a feature that allows rare-earth barium copper oxide (REBCO) HTS tapes to be simply stacked without twisting or transposition. This could be feasible owing to the high cryogenic stability of HTS conductors, which may allow the formation of non-uniform current distribution among the REBCO tapes. In

the STARS conductor, a stack of REBCO tapes is embedded into a copper stabilizer, covered by a stainless-steel jacket with laser beam welding. This configuration primarily assures robust coil winding against intense electromagnetic forces. A 6-m sample of the 20-kA class STARS conductor was fabricated with a 600-mm diameter in a solenoid coil shape of three turns, and tested at a NIFS facility equipped with a maximum magnetic field of 13-T, 700-mm bore coil. A stable operation up to 18 kA current was confirmed at 8 T and 20 K temperature. During the experiment, a residual magnetic field was clearly observed after the transport current was ramped down to zero. A numerical calculation code has been developed for simulating the circulation currents caused by a variation of self-inductances among the simply-stacked HTS tapes, and the measured residual magnetic field was well simulated. It is shown that some of the tape currents reached the critical current at a fast ramp rate without causing an avalanche of normal-transition from tape to tape, which proves stable repetitive excitations with a 1 kA/s ramp rate. Based on these results, the applicability of the simply-stacked HTS conductor to large magnets seems plausible.

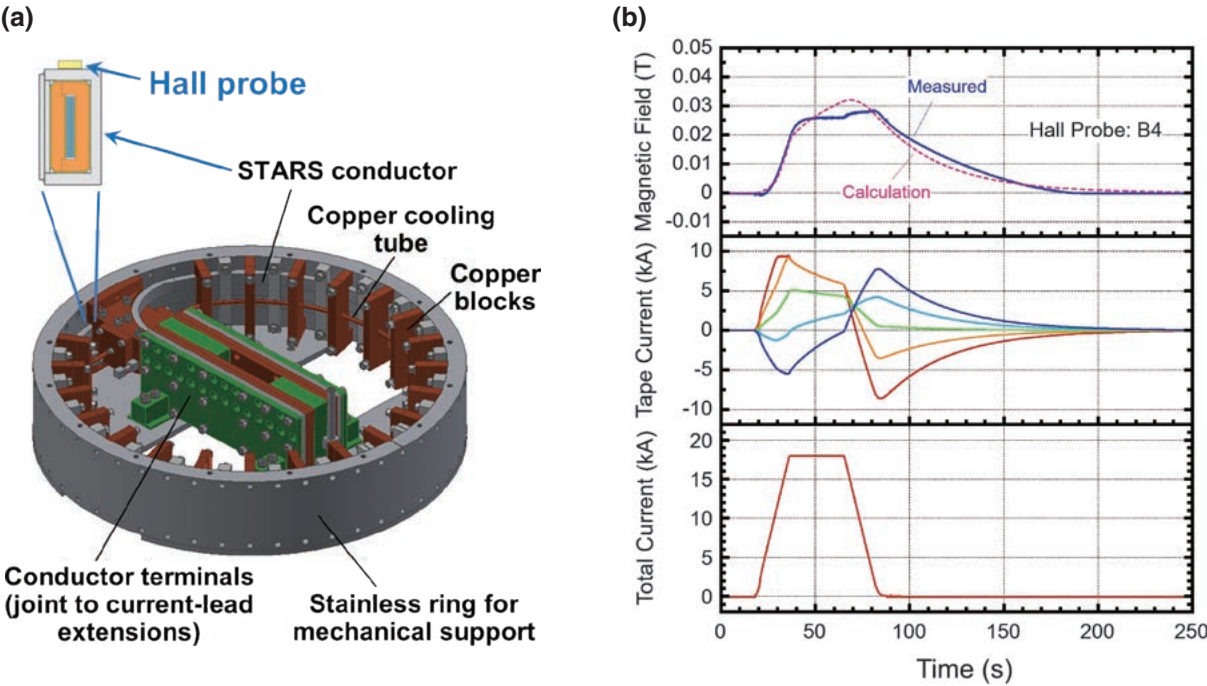


Fig. 2 (a) Schematic illustration of the 6-m, 3-turn-solenoid 20-kA-class STARS conductor sample, indicating also a Hall probe attachment for measuring the magnetic field. (b) Comparison between the measured magnetic field and the numerically calculated one. For the numerical calculation, the STARS conductor, with 15 tapes, is assumed to have five tapes, and the waveforms of the currents in each tape are shown in the middle. The waveform of the sample (total) current with a trapezoidal excitation is shown at the bottom.

(N. Yanagi)